Climate-related Risk Premium and Spillovers

Thomas Giroux*, Julien Royer†

March 2022

Abstract

The growing demand in sustainable investment has fostered numerous changes in the financial industry. Divestment in carbon intensive industries and preference for Green assets should impact classical Asset Pricing models while the contagion effects from Brown to Green assets need to be carefully monitored. In this paper, we leverage Dynamic Factor Models to better quantify Climate-related Risk premium and develop a novel two-step procedure to estimate volatility spillovers between long-only portfolios. This new procedure allows to uncover the high persistence of Brown volatility innovations on Green volatility.

Keywords: Climate Risk, Carbon Risk, Sustainable Investing, Asset Pricing Models, Dynamic Factor Models, Volatility Spillovers

PRELIMINARY WORK, PLEASE DO NOT CITE

*CREST, ENSAE and Institut Polytechnique de Paris, 5 Avenue Henry Le Chatelier, 91120 Palaiseau, France; E-mail: thomas.giroux@ensae.fr

†CREST, ENSAE and Institut Polytechnique de Paris, 5 Avenue Henry Le Chatelier, 91120 Palaiseau, France; E-mail: julien.royer@ensae.fr

1 Introduction

The fast development of Green Investing has spurred academic interest in the impact of climate-related risks on financial returns. However, findings are often contradictory. On the one hand, Pástor et al. [2020] and De Angelis et al. [2020] argue that exposure to climate-related risks should be rewarded by a risk premium while the utility gained by sustainable investors for holding Green stocks compensates the expected lower returns. In addition, Bolton and Kacperczyk [2020] show empirically that firms' carbon intensity is linked to higher returns. On the other hand, in recent years, sustainable assets have outperformed assets with high carbon exposures. Pastor et al. [2021] argue that this outperformance is due to unexpected higher environmental concerns among investors. Therefore, the aggregated effect of climate-related risks over the cross-section of returns is yet unclear. Part of this issue lies in the fact that sustainable preferences are evolving among investors. Awareness about climate change and its consequences is growing along with new scientific findings and political will. Krueger et al. [2020] outline that institutional investors consider climate change as a growing risk in the market. Such transition needs to be taken into account when running econometric analysis. Additionally, managing the financial risks at stake is another issue for asset managers. Indeed, the effects of climate change are widely but unequally spread across sectors and geographies as it may impact firms through various channels (physical, regulatory, reputation). Hence, climate-related risks are hardy diversifiable and might impact financial stability. To that extend, Engle et al. [2020] developed dynamic hedging strategies against climate-related risks. However, a vast majority of sustainable strategies invest in long-only portfolio, prohibiting short selling. There is no evidence that the resulting strategies are hedged against contagion effects from Brown stocks. Hence, besides challenging the existence of a dynamic climate-related risk premium, it appears of primary importance to understand spillover effects between Green and Brown companies, in order to assess the true exposure to climate-related risks of long-only sustainable strategies.

This papers contributes to the literature in two main aspects. First, we investigate the existence of a climate-related risk premium with robust dynamic modeling, allowing to capture the increasing shift in investors preferences toward a more sustainable economy. While most of the literature analysing this issue relies on panel analysis [Bolton and Kacperczyk, 2020, Pastor et al., 2021, Sautner et al., 2021] or standard Fama-MacBeth two steps regression [Görgen et al., 2019], we make use of state of the art conditional beta modeling and follow Gagliardini et al. [2016] to compute a dynamic risk premium. Secondly, we extend the spillover analysis to long only sustainable strategies while it is narrowed to green energy index and sectors in the existing literature. We propose a novel two-step procedure to evaluate accurate climate-related risks contagion effects

between Brown and Green companies. We achieve this by relying on a Autoregressive Conditional Beta model (ACB) introduced by Blasques et al. [2022]. It allows to directly specify and estimate dynamic conditional factor loadings. This proves useful to extend the standard 2-Pass Cross-Sectional Regression approach of Fama and MacBeth [1973] and compute dynamic risk premia following Gagliardini et al. [2016]. Indeed, wrongfully assuming the constancy of slope coefficients in linear regression may lead to erroneous conclusions as underlined by Engle [2016] and numerous models have established the need for time varying parameters in asset pricing models (see for example Gagliardini et al. [2016] or Grassi and Violante [2021]). We find a positive significant risk premium associated with the GMB factor. This results is in lines with empirical findings of Bolton and Kacperczyk [2020] and Pastor et al. [2021]. However, recovering a significant risk premium for the GMB factor is new in the literature as Görgen et al. [2019] did not find significant results using the standard Fama-MacBeth two-steps approach. The value of the GMB risk premium differs depending on the metrics used to build the GMB factor. Tangible and transparent metrics appear to be key to be priced in the market. However, favoring a complete analysis of firms' total exposure to climate-related risks, for instance combining carbon footprint with environmental high-stake sectors classification allows to find higher risk premium than solely focusing on carbon intensity. In addition, we rely on the the ACB model to dynamically hedge long-only portfolio returns of Green and Brown companies against standard risk factors. Following Conrad and Karanasos [2010], the resulting returns are then modelled through a bivariate unrestricted ECCC (uECCC) GARCH to compute volatility spillovers and assess both their level and persistence. Our methodology is able to capture spillovers from Brown to Green assets that cannot be uncovered by simply looking at the unhedged portfolios.

Accordingly, these results argue in favour of an increasing shift of investors preferences toward a more sustainable economy. However, a comprehensive analysis of firms' exposure to climate-related risks, with tangible and easy understandable metrics is required to fully capture and manage financial risks related to climate change. Thus, it is of primary importance to develop standardised approaches and transparent metrics of firms' exposure to climate-related risks.

The paper is structured as follows. Section 2, presents the data used to conduct our analysis and details the construction of potential Green Minus Brown (GMB) factors. Section 3 introduces the dynamic autoregressive conditional betas model (ACB) and assesses the existence of a climate-related risk premium. Section 4 explains how climate-related risk spillovers can be uncovered from ACB model and expose the results on long-only portfolios. Finally Section 5 concludes. Technical details on the conditional

volatility models and the estimators used in the paper are given in the appendix.

2 Data and Climate risk factor

2.1 Data

Estimating risk premium following the Fama and MacBeth [1973] two-step procedure is commonly done on portfolios to reduce the error variances issue. Threfore we use the Fama-French thirty-eight industries portfolios to regress against well known three factors, Market (Mkt), Size (SMB) and Value (HML) obtained on Kenneth R. French 's Data Library [Fama and French, 1993]. We analyse a period of 21 years from 01/01/2000 until 31/12/2020.

Although monthly returns are regularly chosen when estimating risk premium, we use weekly observations to increase the amount of observations as it is of critical importance to accurately estimate dynamic conditional betas. This has been proven to allow for proper estimations in similar asset pricing models [Ferson et al., 1987, Lo and Wang, 2006, Lewellen and Nagel, 2006]. In addition to the classical three factors we introduce an additional climate-related risk factor (hereafter referred to as Green Minus Brown - GMB). As climate-related risks are unobservable, we test multiple candidates to assess the robustness of our results.

2.2 GMB candidates

We follow the mimicking portfolio approach of Fama and French [1993] also adopted by Görgen et al. [2019], Bolton and Kacperczyk [2020], Pastor et al. [2021] to build GMB candidates as zero-cost portfolios long on Green stocks and short on Brown ones.

Carbon emissions is a critical component of firms' exposure to climate-related risks, because of the transitional channel. We collect carbon emissions with Scope 1 to 3 from two different provider, *TruCost* and *Carbone4*. According to the GHG Protocol Corporate Standard [1] *"company's GHG emissions [are divided] into three scopes. Scope 1 emissions are direct emissions from owned or controlled sources. Scope 2 emissions are indirect emissions from the generation of purchased energy. Scope 3 emissions are all indirect emissions (not included in scope 2) that occur in the value chain of the reporting company, including both upstream and downstream emissions."* However, it might not be enough to capture companies' full exposure to climate-related risks as it also depends on firms' overall transition strategic plan and physical exposure to either climate

[1] https://ghgprotocol.org/sites/default/files/standards_supporting/FAQ.pdf

disaster or unexpected change in the process toward sustainable development. Hence, we enhance the data with additional sources. First, *"avoided emissions"* computed by *Carbone4* within the *Net Zero Initiative* project. It assesses companies' contributions to decarbonisation by computing the difference between direct carbon emissions and a reference scenario. Different from *"Negative emissions"*, it encourages organisations to reduce their direct emissions either as a result of the products and services sold or through financing emission reduction projects outside of the value chain. In addition, we collect environmental scores from *ISS* covering a wider range of environmental issues than carbon emissions only. Following recommendations of TCFD [2017] we standardise carbon emissions by year-end net revenues to build carbon intensity metrics that are comparable between companies. To build mimicking portfolios in a consistent manner with Kenneth R. French 's Data Library we use the Center for Research in Security Prices (CRSP) database to collect daily returns from US companies over the same 20 years period. We then restrain the analysis to companies that exist over the entire period and for which carbon data is available. This results in a final sample of 1241 companies out of 18800 in the original CRSP database from which 3328 are matching the carbon database, but not all surviving the entire period. It accounts for 57% of the total market capitalisation on yearly average during the period, meaning that the remaining companies are mostly large capitalisation compared to the full sample available in the CRSP database. 70% of the S&P 500 constituents are present in the final sample with a slight bias in proportion toward Industrials and Financials and less IoT, Health-Care and Communication Services (see table 1). However, this is not a major issue for the construction of GMB candidates since the former sectors are not high-stakes sectors in terms of environmental transition [2].

Carbon emissions are observed at a yearly frequency over the period. As table 1 shows, according to TruCost's data, there has been a continuous decrease in carbon intensity between 2000 and 2020 for all sectors.
Some observations are missing, mostly before 2016 (between 50% and 60%) but it mainly concerns low-stakes sectors in terms of environmental transition. In addition, the ranking of companies is stable across time.

The two carbon datasets differ in absolute value. For instance, the high carbon intensity of Utilities in the *TruCost* dataset differs from the estimation of *Carbone4* due to some companies exposed to Brown electricity production that have lower scope 3 carbon intensity in the *Carbone4* database. However, the two sources show similar ranking results. Therefore it should lead to consistent findings. It differs much more when looking at

[2]Details about high and low-stakes sectors are provided in Hoepner et al. [2019]

	S&P500 (%)	Sample (%)	2000-2007	2008-2012	2013-2016	2016-2020
Communication Services	10.8	1.13	83.76	86.55	86.21	87.78
Consumer Discretionary	12.8	16.12	253.22	222.17	202.15	220.20
Consumer Staples	5.6	5.32	683.75	570.03	517.52	536.94
Energy	2.9	3.95	815.91	749.78	780.92	734.20
Financials	11.4	18.94	49.93	46.44	54.10	45.10
Health Care	13	7.57	169.37	138.88	125.17	130.39
Industrials	8	17.16	395.58	365.24	348.21	345.80
Information Technology	27.9	13.54	181.83	172.20	157.22	150.81
Materials	2.5	6.04	1196.32	1170.31	977.69	996.82
Real Estate	2.6	5.96	169.75	140.64	137.07	129.64
Utilities	2.4	4.27	4344.39	3671.57	3434.72	2604.45

Table 1: Sector distribution & Average scope 3 carbon intensity

the environmental score. Indeed, the environmental score captures a broader picture of the companies' environmental footprint than carbon emissions only. Hence, companies with the same carbon intensity may have different environmental scores (see Figure 1). Berg et al. [2019] highlighted this issue about the divergence of ESG ratings between providers even though descriptions look alike.

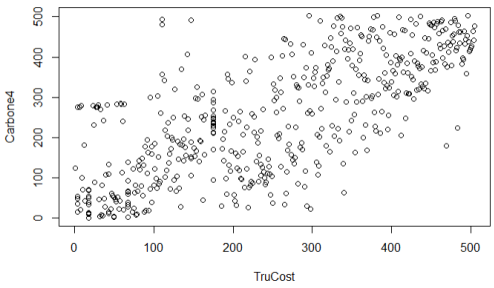

(a) Carbon intensity rankings: TruCost vs. Carbon4

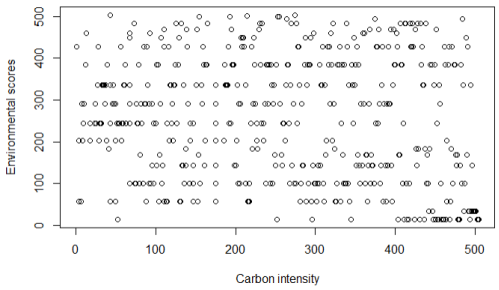

(b) Rankings: Carbon intensity vs Environmental Scores

Figure 1: Carbon data coherence

Finally, we define a low/high-stakes variable for the industries based on carbon intensity. High-Stakes industries are those in the fourth quartile of carbon emissions intensities. This approaches leads to similar results than high-stakes sectors define in Hoepner et al. [2019].

Unlike environmental scores, there is no linear link between carbon intensity (in both sources) and firm valuation such as Price to Book ratio (P2B) and market capitalisation. The higher the environmental score, the higher the valuation of the companies and the faster this valuation grows over time.

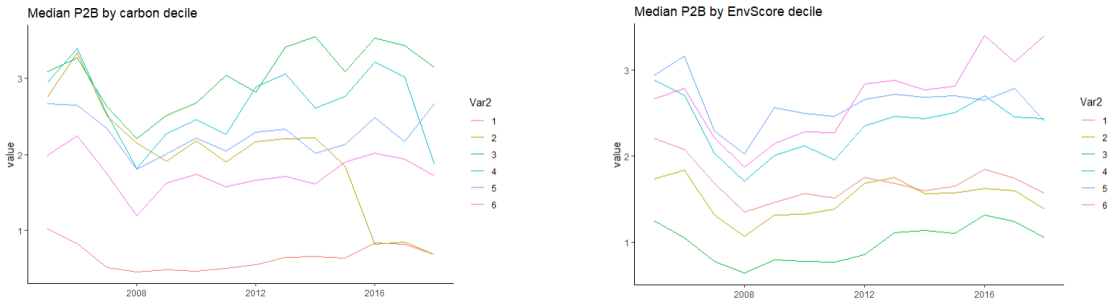

(a) Deciles Carbon TruCost

(b) Deciles Environmental Score ISS

Figure 2: Price to Book evolution by decile

Even though the average carbon intensity decreased during the last 10 years, the ranking between companies remained mostly unchanged (see Table 2). Furthermore, since Scope 3 methodology has evolved through time and more and more companies are disclosing their carbon footprint each year, we use only last available observations to distinguish Green from Brown companies. This is especially convenient as it allows to have stable groups of Green and Brown companies across time.

	2005	2010	2016
2005	1.00	0.91	0.89
2010	0.91	1.00	0.97
2016	0.89	0.97	1.00

Table 2: TruCost carbon rankings correlations

Following standard practices in sustainable investing [Statman, 2006, Kempf and Osthoff, 2007], two possible methods may be implemented to screen GMB portfolio candidates: *Best-in-Universe (BinU)* & *Best-in-Class (BinC)*. *Best-in-Universe* aims to select companies with best/worst environmental metrics in the throughout the universe while *Best-in-Class* screens companies with best/worst environmental metrics within each sector or industry. The first may lead to over-exposition of one class meanwhile the other requires well distributed data among the classes. In order to recover robust results, we apply both approaches on all environmental metrics available and compute multiple GMB candidates. When considering carbon intensity only, the two screening methods lead to diverse outcomes. On the one hand, BinU GMB portfolios have a Green leg over-exposed to the finance sector and in smaller proportions to health-care and IoT. Hence, a bias appears toward sectors either with inappropriate carbon emissions accounting [CDP, 2020] or with little contribution to the environmental transition. It is thus excluded from further analysis. On the other hand, BinC approaches and BinU with an additional filter on high-stakes industries lead to well diversified portfolios with Green and Brown companies in almost all sectors or sectors with high impact on fighting

climate change. This is in line with the recommendations of the European Commission Technical Expert Group (TEG) on Paris Aligned Benchmarks (PAB) [Hoepner et al., 2019]. Adding avoided emissions to the screening improves the *Best-in-universe* approaches and is done via the average rank between induced emissions and saved ones. It encompasses wider concerns about climate change and leads to well diversified portfolios with natural exposure to high-stakes sectors such as industrials, materials and utilities. Almost no Green companies are found in the energy sectors however since it has very poor avoided emissions on average. Environmental scores also give satisfying portfolios in terms of diversification and weighted-average carbon intensity between Green and Brown companies.

In the upcoming work, we restraint the analysis to four representatives GMB candidates, *GMB1* denotes a factor based on *TruCost* scope 3 carbon intensity and is built following the *Best-in-Class* approach; *GMB2* is constructed with *TruCost* scope 3 carbon intensity and screened throughout the Universe of High-Stake sectors; *GMB3* corresponds a portfolio based on *ISS* environmental scores with a *Best-in-Universe* screening; and finally, *GMB4* which is built following a *Best-in-Universe* screening on a ratio of *"avoided emissions"* over *"induced emissions"* computed by *Carbone4*. Those four factors share common properties and rely on four dimensions of climate-related risks each one embracing a different range of climate-related issues.

First of all, every Green leg has higher monthly average return and higher Sharpe ratio than its Brown counterpart. The long-short performance of GMB varies between each approach however but all of them show positive compound returns after 2010, with different proportions. Only GMB4 built upon induced and saved emissions achieves a straight out-performance over the period. This yield variation in Sharpe ratio, ranging from -0.017 for GMB3 to 0.209 for GMB4. Hence, GMB1 to GMB3 have lower monthly return on average than SMB or HML. Regarding financial ratios, Green companies are more expensive and bigger than Brown ones. Indeed, the median price to book ratio of Green companies is on average 1.30 times higher than Brown ones while the median market share is on average 2 times higher over the period. Tables 3 and 4 in Appendix A present all details about GMB candidates.

Figure 3 shows the compound returns of the four selected GMB factors as well as the three Fama-French factors.

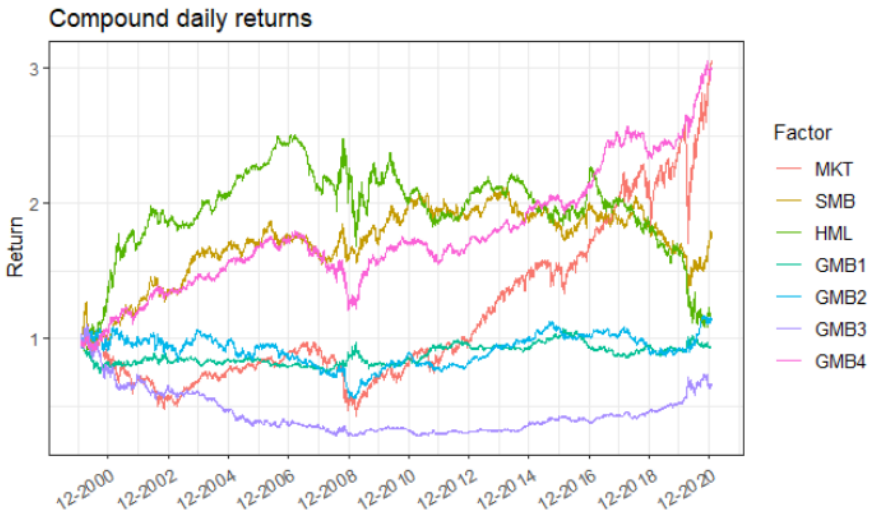

Figure 3: Equity pricing factors of interest

3 Estimating the time-varying risk premium of the Green Minus Brown factor

The pricing of climate-related risks in financial returns is of growing concern in the academic literature. Bolton and Kacperczyk [2020] run large cross-section regressions at the firm level and find a widespread carbon premium that is not well explained by traditional equity pricing factors. Using another definition of climate change exposure Sautner et al. [2021] confirm this findings when looking at proxies of expected returns but not on realised returns. However, both of these studies rely on firms characteristics to build cross-sectional regressions. They do not test for the existence of a risk factor commonly associated with mimicking long-short portfolio returns. Görgen et al. [2019] attempt to do so and find a non-significant risk premium but rely on rolling-window estimators to capture the dynamics of factor loadings. Such estimation technique lies however on erroneous assumptions which makes the test of the existence of a premium hardly conclusive.

3.1 An asset pricing model with time-varying coefficients

Asset pricing models are built on linear regressions where the excess returns of a financial asset are explained by a set of factors. Let us denote $(r_{i,t})$ the excess returns time series of a asset $i = 1, \dots, N$ in a system of N assets and $\boldsymbol{f}_t = (f_{1,t}, \dots, f_{m,t})'$ a set of m observable factors. Usual asset pricing models are thus of the form

$$r_{i,t} = \alpha_i + \boldsymbol{\beta}_i' \boldsymbol{f}_t + \varepsilon_{i,t}$$

where the regression coefficients α_i and $\boldsymbol{\beta}_i = (\beta_{i,1}, \ldots, \beta_{i,m})'$ are assumed to be constant. However, there is no economic rationale for these parameters to be time invariant, and numerous papers actually account for variations in the slope coefficients (see Engle [2016] and references therein). We therefore favor a conditional regression model of the form

$$r_{i,t} = \alpha_{i,t} + \boldsymbol{\beta}_{i,t}{}' \boldsymbol{f}_t + \varepsilon_{i,t}. \tag{1}$$

Practitioners usually obtain time-varying estimates of the regression parameters by computing OLS estimators on rolling windows. However, this method lies on inconsistent assumptions since the obtained estimator targets constant betas on the considered time frame. Engle [2016] proposed to model conditional betas as a transformation of the conditional covariance matrix of a multivariate GARCH model. Although this method provides a direct estimation of the betas after estimating the model (usually using a Dynamic Conditional Correlation GARCH), the variable of interest is not directly specified. Indeed, the conditional betas are obtained from a transformation of the conditional covariance matrix, which makes hypothesis testing on the dynamic betas impractical. In addition, the estimated time-varying coefficients are often highly volatile.

Directly modeling betas dynamics provides numerous advantages as it allows to gain economic and financial interpretability on the time-varying dependency between assets or factors and allows for testing procedures. Gagliardini et al. [2016] proposed to introduce dynamics into the regression coefficient through instrumental variables, following ideas from Ferson and Harvey [1991] among others. The obtained factor loadings are however highly sensitive to the choice of instrumental variables as noted by Ghysels [1998]. Darolles et al. [2018] proposed a new multivariate GARCH model where the conditional betas can be obtained from a Cholesky decomposition of the conditional covariance matrix. However, it requires estimating the full multivariate system even if only one equation is of interest. For example, Equation (1) would require the estimation of m intermediate models, which makes it impractical for an asset pricing exercise where estimation of the equation has to be repeated N times.

To remedy these issues, Blasques et al. [2022] recently proposed a novel model to obtain dynamic betas in the form of Autoregressive Conditional Betas (ACB). This model builds upon the score-driven models literature introduced by Creal et al. [2013] to allow for both time-varying regression coefficients and conditional heteroscedasticity of the factors which is highly relevant in financial applications. In particular, assume that each

factor f_j dynamic is given by a GARCH(1,1) with constant conditional mean

$$\begin{aligned} f_{j,t} &= \mu_j + \sigma_{j,t}\eta_{j,t} \\ \sigma^2_{j,t} &= \omega_j + a_j(f_{j,t-1} - \mu_i)^2 + b_j\sigma^2_{j,t-1} \end{aligned} \tag{2}$$

where $\eta_{j,t}$ is an iid centered random variable with unit variance. Similarly, assume that the residuals of the conditional regression follows a GARCH(1,1) with conditional variance

$$g^2_{i,t} = \omega_{\varepsilon_i} + a_{\varepsilon_i}(r_{i,t-1} - \alpha_{i,t-1} - \boldsymbol{\beta}_{i,t-1}{}'\boldsymbol{f}_{t-1})^2 + b_{\varepsilon_i}g_{i,t-1}. \tag{3}$$

Additionally, assume that the conditional regression parameters follow the autoregressive updating equations

$$\begin{aligned} \alpha_{i,t+1} &= \overline{\omega}_{\alpha_i} + \xi_{\alpha_i}\varepsilon_{i,t} + c_{\alpha_i}\alpha_{i,t} \\ \beta_{i,j,t+1} &= \overline{\omega}_{i,j} + \xi_{i,j}\frac{f_{j,t}\ \varepsilon_{i,t}}{\mu^2_j + \sigma^2_{j,t}} + c_{i,j}\beta_{i,j,t} \end{aligned} \tag{4}$$

for $i = 1, \ldots, N$ and $j = 1, \ldots, m$.

These dynamics are obtained from a Gaussian score-driven updating equation as presented in Appendix C. Note that, although derived from technical assumptions, the updating term $f_{j,t}\varepsilon_{i,t}/(\mu^2_j + \sigma^2_{j,t})$ is very intuitive. Indeed, if $\xi_{i,j}$ and $c_{i,j}$ are positive, the term $f_{j,t}\varepsilon_{i,t}$ implies that the update attempts to obtain beta values for which the residuals $\varepsilon_{i,t}$ are not only unconditionally orthogonal to the factor f_j as usual in linear regressions, but also conditionally orthogonal. Additionally, as the updating term is inversely proportional to the conditional volatility $\sigma^2_{j,t}$, the updating step size is less important in period of high volatility, ensuring less noisy conditional betas. The updating equation of the intercept $\alpha_{i,t}$ is similar to the betas equation, except that since the related factor is constantly equal to one, its variance is null, thus the denominator of the updating term is equal to one. All parameters can easily be inferred by Quasi Maximum Likelihood (QML) and asymptotic results are presented in Appendix D.

To conclude the definition of our dynamic asset pricing model, we follow Gagliardini et al. [2016]. Under standard assumptions linked to the absence of arbitrage opportunities, asset pricing models with time-varying factor loadings verify that, for any t, there exists a unique random vector $\boldsymbol{v}_t = (v_{1,t}, \ldots, v_{m,t})'$ such that for almost all i,

$$\alpha_{i,t} = \boldsymbol{\beta}_{i,t}{}'\ \boldsymbol{v}_t \quad \text{almost surely.} \tag{5}$$

The dynamic asset pricing model (1) combined with (5) yields that for almost all i,

$$\mathbb{E}[r_{i,t}|\mathcal{F}_{t-1}] = \boldsymbol{\beta}_{i,t}{}' \, \boldsymbol{\lambda}_t \quad \text{almost surely,} \tag{6}$$

where $\boldsymbol{\lambda}_t$, the vector of time-varying risk premia, is given by $\boldsymbol{\lambda}_t = \boldsymbol{v}_t + \boldsymbol{\mu}$ with $\boldsymbol{\mu} = \mathbb{E}[\boldsymbol{f}_t] = (\mu_1, \ldots, \mu_m)$. For example, in the CAPM, we have $\boldsymbol{v}_t = 0$.

The estimation of time invariant risk premia is usually conducted using Fama and MacBeth [1973] procedure. In that spirit, Gagliardini et al. [2016] proposed a two-step procedure to infer dynamic risk premia. We draw from the latter to propose the following two step procedure to recover time-varying risk premia from the ACB model. The first step consists in the estimation of $\alpha_{i,t}$ and $\boldsymbol{\beta}_{i,t}$ by QML, for each asset i in the system, $i = 1, \ldots, N$. The second step deals with the estimation of $\boldsymbol{v}_t$ from the cross section of assets. For each t, we estimate this vector from (6) by regressing $\boldsymbol{\alpha}_t = (\alpha_{i,t})_{i=1,\ldots,n}$ on $\boldsymbol{\beta}_t = (\boldsymbol{\beta}_{i,t})_{i=1,\ldots,n}$ using OLS. Combining $\boldsymbol{v}_t$ with parameter $\boldsymbol{\mu}$ estimated in the first step yields the time-varying risk premia $\boldsymbol{\lambda}_t$.

3.2 Does the GMB factor matter in the regression of stock returns?

To assess the existence of a risk premium associated to climate related risks, we consider $r_{i,t}$ the weekly excess returns of the 38 industries portfolio and the three standard Fama-French factors to which we add a GMB factor: $\boldsymbol{f}_t = (\text{Mkt}_t, \text{HML}_t, \text{SMB}_t, \text{GMB}_t)'$. In order to highlight the benefits of using our proposed ACB pricing model, we compare our results to the benchmark procedure of rolling Fama-MacBeth procedure.

Figure 4 illustrate dynamic betas of GMB built on environmental score (GMB3) for two industries, Oil and Gas Extraction and Retail. While the Oil and Gas Extraction industry experiences large increase in its sensitivity to climate-related risks, the retail industry shows varying but positive exposure to the GMB factor. This illustrates the increasing awareness about the challenges faced by the fossil fuel industry due to climate change while the retail industry is not of high-stakes in the ecological transition.

Dynamic betas obtained from the first step of our procedure share similat features with OLS estimates computed on a fixed 3-year window in terms of trends, magnitudes and rankings to the GMB candidates. Details are given in Appendix B though Tables 5 to 9. Conditional betas are however less volatile than the one recovered from rolling windows regressions. Table 10 in Appendix B provides more details. This argues in favor of the Autoregressive Conditional Beta (ACB) model to improve the dynamic factor loadings estimation and thus reduces errors when computing the risk premium. Applying our

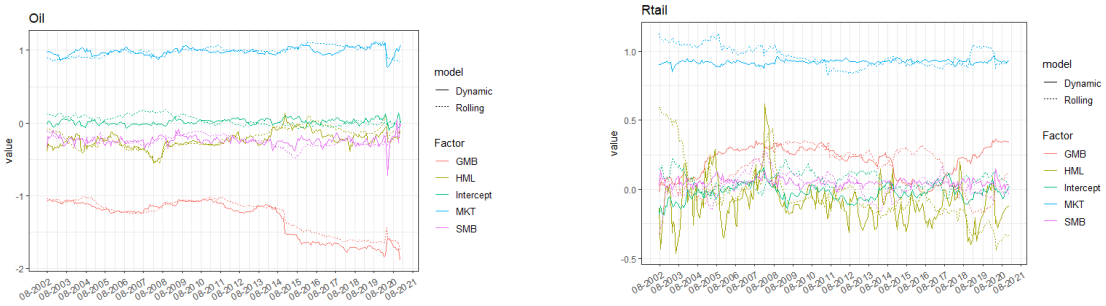

(a) Oil and Gas Extraction

(b) Services

Figure 4: Conditional Betas

two-step procedure allows to recover significant risk premium of around 4% annualised for the market in every model. Additionally, the GMB factor risk premium is significant for all GMB candidates except GMB3, with values of ranging from 1.3% to 4% annually. Details are given in appendix B in Table 11. It clearly differs from the outcome of the Fama-MacBeth procedure giving no statistically significant risk premium for any of the equity pricing factors, including the GMB candidates. This supports the need for proper dynamic beta modeling and time varying risk premium estimates.

Moreover, this new result in the literature underlines the overperformance of Green stocks over Brown ones and confirms the ability of climate-related risks to explain the cross-section of returns. The clear dynamic of the GMB risk premium, shown in Figure 5 strengthens our approach compared to the static standard Fama-MacBetch procedure. One can observe an increasing risk premium in times of bull markets, for instance after the 2008 crisis or when climate attention is at a peak, (e.g after the 2016 COP 21) and turning negative in times of financial crises. Also, a significant difference in magnitude appears between GMB candidates. Especially, *GMB2*, based on High-Stake industries, delivers higher but more volatile risk premium. This result underlines the importance of managing climate-related risks with several metrics, encompassing a wide range of issues and favouring tangibility and transparency over black-box approaches to ease market acceptance and pricing.

4 Volatility spillovers between Green and Brown Portfolios

Assessing the connection between Green and Brown stocks has become central in the financial industry as demand for sustainable investment grows. In particular, as some investors have long-only constraint, it is crucial to measure the contagion from climate-related risks to Green assets. On that matter, Henriques and Sadorsky [2008] and Bondia et al. [2016] study the connection between Oil prices and clean energy stocks returns.

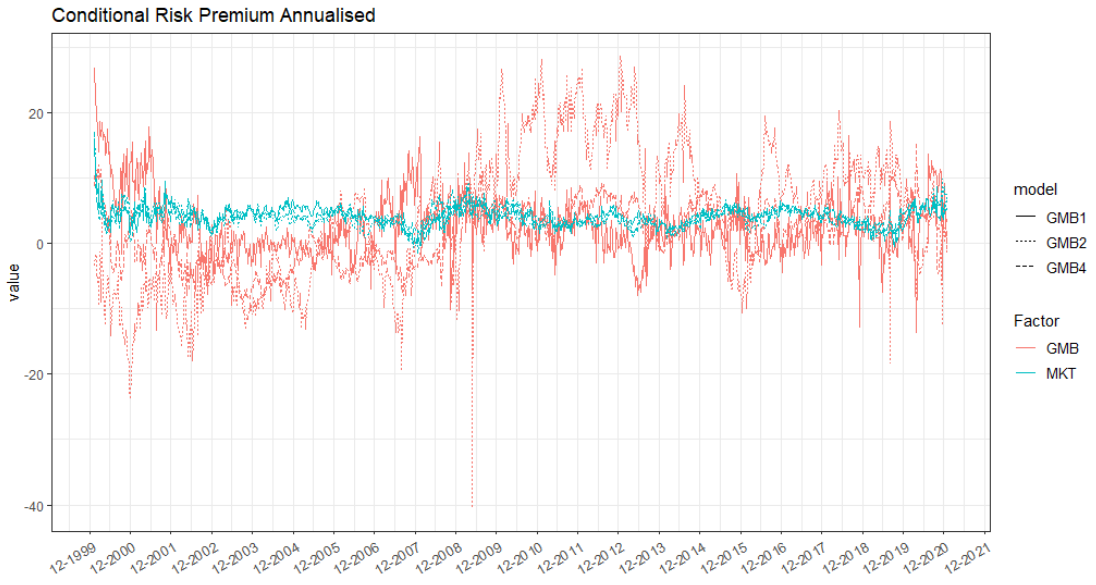

Figure 5: Conditional risk premium

However, their work only focuses on a particular sector and do not investigate spillovers from Brown stocks. Recently, Nobletz et al. [2021] investigated the interconnection between clean energy indexes and sector portfolios. Alternatively, we model directly the volatility spillovers between Green and Brown portfolios which allows for a more interpretable contagion measure of volatility innovations stemming from climate-related risks.

Surprisingly, to the best of our knowledge, most spillover analysis on climate-related risks have been conducted on carbon risk solely, using the methodology of Diebold and Yılmaz [2014] based on the Generalized Variance Decomposition of Koop et al. [1996] in VAR models. Linear models may not be the most adequate framework when studying financial volatilities and we propose to use multivariate GARCH models instead. Such models allow for a decomposition of the conditional variance of an asset between individual effects and cross effects stemming from other assets in the system. Let us denote $\boldsymbol{r}_t = (r_{\mathrm{B},t}, r_{\mathrm{G},t})'$ with $r_{\mathrm{B},t}$ and $r_{\mathrm{G},t}$ the returns of the Brown and Green portfolios respectively. We consider a general multivariate conditional volatility model

$$\boldsymbol{r}_t = \boldsymbol{\Sigma}_t^{1/2}\boldsymbol{\eta_t}, \quad \boldsymbol{\Sigma}_t = \boldsymbol{H}_t\boldsymbol{R}_t\boldsymbol{H}_t$$

where $(\boldsymbol{\eta}_t)$ is a sequence of independent and identically distributed random vectors with zero mean and identity covariance matrix and $\boldsymbol{H}_t = \mathrm{diag}\{\boldsymbol{g}_t^{1/2}\}$ the diagonal matrix of individual conditional volatilities, $\boldsymbol{g}_t = (g_{\mathrm{B},t}, g_{\mathrm{G},t})'$, and $\boldsymbol{R}_t$ a correlation matrix measurable with respect to the sigma-field $\{\boldsymbol{r}_u, u < t\}$. In particular, a very general model

for $\boldsymbol{g}_t$ is the Extended Constant Conditional Correlation (ECCC) GARCH model of Jeantheau [1998] given by

$$\boldsymbol{g}_t = \boldsymbol{\omega} + \sum_{i=1}^{q} \boldsymbol{A}_i \boldsymbol{r}_{t-i}^2 + \sum_{j=1}^{p} \boldsymbol{B}_j \boldsymbol{g}_{t-j}. \tag{7}$$

More precisely, we consider the *unrestricted* ECCC (uECCC) GARCH model of Conrad and Karanasos [2010] relaxing the hypothesis of positivity of the off-diagonal terms in $\boldsymbol{B}_j$ allowing for possibly negative GARCH spillovers. This model is particularly suited for the analysis of volatility contagion as spillovers can easily be derived from the off-diagonal elements of the matrices $\boldsymbol{A}_i$ and $\boldsymbol{B}_j$. Indeed, consider a bivariate uECCC-GARCH(1,1) model, we obtain the following equation for the conditional variance vector

$$\begin{bmatrix} g_{\mathrm{B},t} \\ g_{\mathrm{G},t} \end{bmatrix} = \begin{bmatrix} \omega_1 \\ \omega_2 \end{bmatrix} + \begin{bmatrix} a_{11} & a_{12} \\ a_{21} & a_{22} \end{bmatrix} \begin{bmatrix} r_{\mathrm{B},t-1}^2 \\ r_{\mathrm{G},t-1}^2 \end{bmatrix} + \begin{bmatrix} b_{11} & b_{12} \\ b_{21} & b_{22} \end{bmatrix} \begin{bmatrix} g_{\mathrm{B},t-1} \\ g_{\mathrm{G},t-1} \end{bmatrix}$$

which yields

$$\begin{cases} g_{\mathrm{B},t} = & \omega_1 + \overbrace{a_{11} r_{\mathrm{B},t-1}^2 + b_{11} g_{\mathrm{B},t-1}}^{\text{Brown own effect}} + \overbrace{a_{12} r_{\mathrm{G},t-1}^2 + b_{12} g_{\mathrm{G},t-1}}^{\text{Green spillover}} \\ g_{\mathrm{G},t} = & \omega_2 + \underbrace{a_{22} r_{\mathrm{G},t-1}^2 + b_{22} g_{\mathrm{G},t-1}}_{\text{Green own effect}} + \underbrace{a_{21} r_{\mathrm{B},t-1}^2 + b_{21} g_{\mathrm{B},t-1}}_{\text{Brown spillover}} \end{cases}$$

Following Conrad and Karanasos [2010] and Conrad and Weber [2013], we rewrite model (7) in terms of volatility innovations $\boldsymbol{h}_t := \boldsymbol{r}_t^2 - \boldsymbol{g}_t$ such that $\mathbb{E}[\boldsymbol{h}_t | \mathcal{F}_{t-1}] = 0$. In that case, a volatility shock $r_{i,t}^2$ can imply a positive or negative volatility innovation depending on whether it is larger or smaller than expected. The model yields

$$\begin{cases} g_{\mathrm{B},t} = & \omega_1 + \overbrace{a_{11} h_{\mathrm{B},t-1} + (a_{11} + b_{11}) g_{\mathrm{B},t-1}}^{\text{Brown own effect}} + \overbrace{a_{12} h_{\mathrm{G},t-1} + (a_{12} + b_{12}) g_{\mathrm{G},t-1}}^{\text{Green spillover}} \\ g_{\mathrm{G},t} = & \omega_2 + \underbrace{a_{22} h_{\mathrm{G},t-1} + (a_{22} + b_{22}) g_{\mathrm{G},t-1}}_{\text{Green own effect}} + \underbrace{a_{21} h_{\mathrm{B},t-1} + (a_{21} + b_{21}) g_{\mathrm{B},t-1}}_{\text{Brown spillover}} \end{cases}$$

Interestingly, this model allows not only to measure spillovers as the initial impact of foreign volatility innovations (captured by coefficients a_{12} and a_{21}), but also to model spillovers persistence. Let us denote for $i, j \in \{\mathrm{B}, \mathrm{G}\}$, $k = 1, 2, \ldots,$

$$\lambda_{ii,k} = \frac{\partial g_{i,t}}{\partial h_{i,t-k}} \text{ and } \lambda_{ij,k} = \frac{\partial g_{i,t}}{\partial h_{j,t-k}}.$$

Coefficients $\lambda_{ij,k}$ can thus be interpreted as the effect on the conditional variance of asset i, $g_{i,t}$, of an own volatility innovation $h_{i,t-k}$, or a foreign volatility innovation $h_{j,t-k}$, at

time $t-k$. The computation of these coefficients follows from Conrad and Karanasos [2010] and is detailed in Appendix E.

4.1 Long-only Green and Brown portfolios

We first investigate the relationship between long-only Green and Brown portfolios volatilities. Figure 6 present the track and conditional volatilities of the two portfolios formed on *TruCost* scope 3 carbon intensity and built following the *Best-in-Class* approach. Of course, both portfolios being long equities, they appear highly correlated.

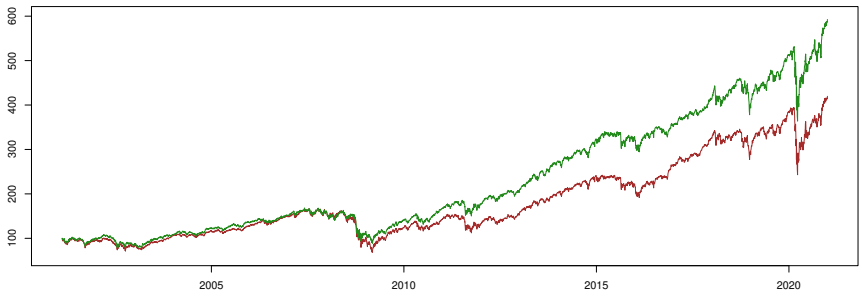

(a) *Portfolio tracks*

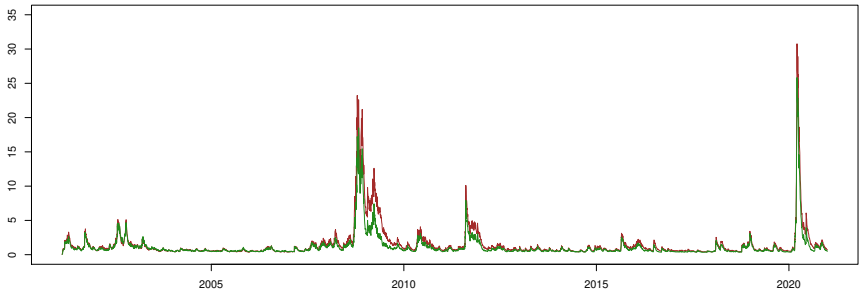

(b) *Conditional volatilities*

Figure 6: *Performance and volatilities of the Green (green line) and Brown (brown line) portfolios.*

We fit a bivariate uECCC-GARCH(1,1) on the returns. The QML estimator yields

$$\begin{bmatrix} g_{\mathrm{B},t} \\ g_{\mathrm{G},t} \end{bmatrix} = \begin{bmatrix} 0.037 \\ 0.033 \end{bmatrix} + \begin{bmatrix} 0.038 & 0.039 \\ 0.013 & 0.056 \end{bmatrix} \begin{bmatrix} r^2_{\mathrm{B},t-1} \\ r^2_{\mathrm{G},t-1} \end{bmatrix} + \begin{bmatrix} 0.964 & -0.089 \\ 0.000 & 0.888 \end{bmatrix} \begin{bmatrix} g_{\mathrm{B},t-1} \\ g_{\mathrm{G},t-1} \end{bmatrix}$$

with a constant conditional correlation of 91.2%. We first notice that both Green and

Brown portfolios impact each others volatilities. Interestingly, we note that the initial impact of Green portfolio volatility innovations on the Brown portfolio is higher than the effect of Brown portfolio volatility innovations on the Green portfolio as $a_{12} > a_{21}$. This indicates a higher immediate impact of the spillover effect stemming from Green returns than from Brown returns. Additionally, Figure 7 presents the response functions to volatility innovations $\boldsymbol{h}_{t-k}$ for $k = 1, \ldots, 100$. We remark that the Green portfolio volatility appears less persistent than the Brown's. Indeed, we clearly see the fastest decay of the response functions as the number of lags increases for the Green portfolio. Besides, the spillover effect from Green to Brown is less persistent than the effect of Brown returns own volatility innovations. Finally, one can remark that even though the volatility contagion from Brown to Green is low, it is persistent, due to the positive parameter b_{21}.

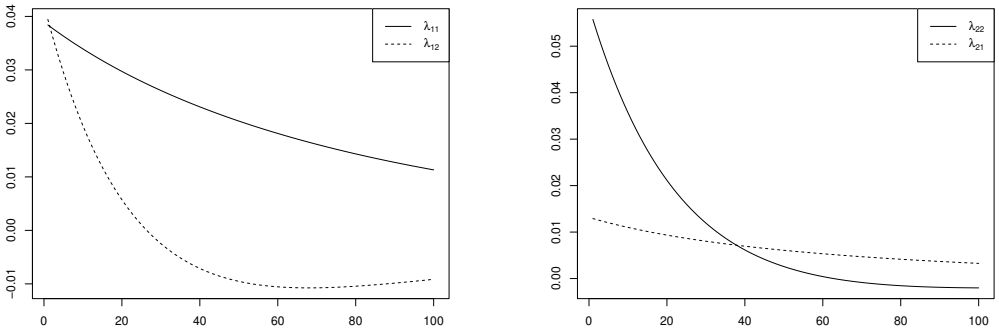

(a) *Response function of* $g_{B,t}$ (b) *Response function of* $g_{G,t}$

Figure 7: *Response functions of the conditional volatilities of Brown and Green portfolios to volatility innovations.*

4.2 Factor-hedged Green and Brown portfolios

Spillover analysis on long-only portfolios may however carry misleading information on the connection between Green stocks and climate-related risks. Indeed, both the Green and Brown portfolios share expositions to similar factors that render the analysis of variance innovations difficult to attribute to climate-related risks only. For example, both portfolios are exposed to the Equity Market risk, and volatility innovations of this factor will impact both portfolios. The contagion analysis between $g_{\mathrm{G},t}$ and $g_{\mathrm{B},t}$ should thus be corrected to take into account the effect of global Equity factors, thus ensuring that the remaining volatility innovations $h_{\mathrm{B},t}$ relate to climate-related risks.

In order to study the contagion from Brown assets to Green assets, we propose to consider the Brown and Green portfolios hedged from a set of common factors $\boldsymbol{f}_t$. The ACB model presented in Subsection 3.1 is particularly suited to that extent. Indeed, it allows to recover the estimated residuals in the conditional regression (1) which are by construction conditionally orthogonal to the factors $\boldsymbol{f}_t$. We thus propose the following two-step procedure to recover volatility spillovers between two long-only portfolios. In a first step, for each portfolio, compute dynamically beta-hedged portfolios using the ACB model. Let us denote $\mathring{\boldsymbol{v}}_t$ the hedge-portfolios returns. In a second step, fit an uECCC-GARCH(1,1) on $\mathring{\boldsymbol{v}}_t$ to uncover volatility spillovers. Let $\mathring{\boldsymbol{g}}_t$ the vector of individual conditional volatilities of the hedged portfolios.

We consider the benchmark model of Fama and French [1993] and consider the 3 factors $\boldsymbol{f}_t = (\text{Mkt}, \text{SMB}, \text{HML})$. Figure 8 presents the performance and conditional volatilities of the hedged Green and Brown portfolios formed on *TruCost* scope 3 carbon intensity and built following the *Best-in-Class* approach. We clearly see that removing factors exposures allows to obtain uncorrelated returns while the volatilities still appear to share some common dynamics.

The QML estimator of the uECCC GARCH model yields

$$\begin{bmatrix} \mathring{g}_{\text{B},t} \\ \mathring{g}_{\text{G},t} \end{bmatrix} = \begin{bmatrix} 1.7e^{-4} \\ 5.8e^{-4} \end{bmatrix} + \begin{bmatrix} 0.089 & 0.008 \\ 0.037 & 0.026 \end{bmatrix} \begin{bmatrix} v^2_{\text{B},t-1} \\ v^2_{\text{G},t-1} \end{bmatrix} + \begin{bmatrix} 0.709 & 0.098 \\ 0.002 & 0.946 \end{bmatrix} \begin{bmatrix} \mathring{g}_{\text{B},t-1} \\ \mathring{g}_{\text{G},t-1} \end{bmatrix}$$

with a constant conditional correlation of -4.2%. Interestingly, the spillover from Brown to Green portfolio is now higher than the one from Green to Brown portfolio. This result contrasts with the one obtained on unhedged portfolios and gives new insights on the volatility contagion stemming from climate-related risk to Green assets. Moreover, Figure 9 shows that most of the conditional volatility of hedged Green portfolio is driven by Brown portfolio volatility innovations. This effect is both observable in term of initial effect and persistence. Unlike the misleading conclusions of the unhedged analysis, this result highlights that long-only portfolios of Green assets are not fully hedged against climate-related risks affecting Brown assets. This provides a strong argument in favor of our proposed method for enhancing risk management.

Appendix F shows that similar results are found when using portfolios built following a *Best-in-Universe* screening on a ratio of *"avoided"* over *"induced"* emissions computed by *Carbone4* (GMB4). However, when considering portfolios formed on GMB2 and GMB3 criteria, we find no evidence of spillovers from Brown to Green.

(a) *Portfolio tracks*

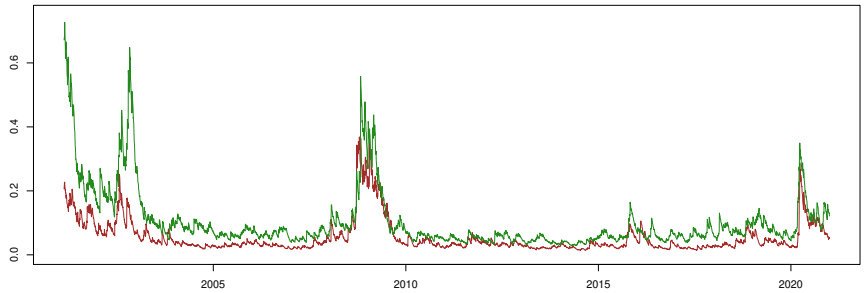

(b) *Conditional volatilities*

Figure 8: *Performance and volatilities of the Hedged Green (green line) and Brown (brown line) portfolios.*

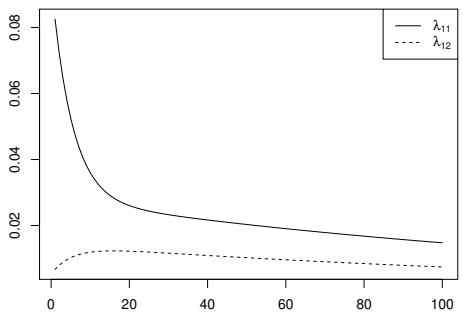

(a) *Response function of* $\mathring{g}_{B,t}$

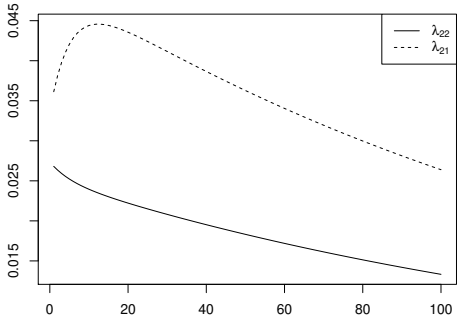

(b) *Response function of* $\mathring{g}_{G,t}$

Figure 9: *Response functions of the conditional volatilities of Brown and Green hedged portfolios to volatility innovations.*

5 Conclusion

The dynamic modeling of the relationship between asset returns and risk factor is crucial when estimating asset pricing models and volatility contagion. In this paper, we leverage the recent Autoregressive Conditional Beta model of Blasques et al. [2022] in two ways. First, we show that direct modeling of dynamic conditional betas yield good estimate of the relationship between stock returns and a Green Minus Brown factor. This is particularly useful as the estimation of slope coefficients is central to recover risk premia in dynamic asset pricing models. Building upon Fama and MacBeth [1973] and Gagliardini et al. [2016], we use a two-step procedure to determine factors risk premia. Our procedure allows us to uncover a significant Carbon-related risk premium, providing new arguments in the question of Green assets outperformance. Additionally, this paper contributes to the analysis of volatility spillovers. We introduce a new procedure to measure volatility contagion. In a first step, we recover the residuals from the ACB model to ensure a dynamic hedging of a set of observable factors. In a second step, we fit an unrestricted ECCC GARCH model on the hedged return series and derive the volatility spillovers and their persistence. The application of this procedure on Green and Brown portfolio provides a strong argument in favor of the proposed model as it allows to uncover a strong and persistent effect of volatility innovations of Brown returns on Green volatility for carbon based portfolios. This contagion effect seems to be lower with Green and Brown portfolios built on environmental scores, advocating for broader metrics of firms climate-related risks exposure for better risk management.

References

F. Berg, J. F. Koelbel, and R. Rigobon. *Aggregate confusion: The divergence of ESG ratings*. MIT Sloan School of Management, 2019.

F. Blasques, C. Francq, and S. Laurent. Autoregressive conditional betas. *Working paper*, 2022.

P. Bolton and M. Kacperczyk. Do investors care about carbon risk? Technical report, National Bureau of Economic Research, 2020.

R. Bondia, S. Ghosh, and K. Kanjilal. International crude oil prices and the stock prices of clean energy and technology companies: Evidence from non-linear cointegration tests with unknown structural breaks. *Energy*, 101:558–565, 2016.

CDP. The time to green finance. Technical report, CDP, 2020.

C. Conrad and M. Karanasos. Negative volatility spillovers in the unrestricted eccc-garch model. *Econometric Theory*, pages 838–862, 2010.

C. Conrad and E. Weber. Measuring persistence in volatility spillovers. *University of Heidelberg, Department of Economics, Discussion Paper*, (543), 2013.

D. Creal, S. J. Koopman, and A. Lucas. Generalized autoregressive score models with applications. *Journal of Applied Econometrics*, 28(5):777–795, 2013.

S. Darolles, C. Francq, and S. Laurent. Asymptotics of cholesky GARCH models and time-varying conditional betas. *Journal of Econometrics*, 204(2):223–247, 2018.

T. De Angelis, P. Tankov, and O. D. Zerbib. Environmental impact investing. *Available at SSRN 3562534*, 2020.

F. X. Diebold and K. Yılmaz. On the network topology of variance decompositions: Measuring the connectedness of financial firms. *Journal of econometrics*, 182(1):119–134, 2014.

R. F. Engle. Dynamic conditional beta. *Journal of Financial Econometrics*, 14(4): 643–667, 2016.

R. F. Engle, S. Giglio, B. Kelly, H. Lee, and J. Stroebel. Hedging climate change news. *The Review of Financial Studies*, 33(3):1184–1216, 2020.

E. F. Fama and K. R. French. Common risk factors in the returns on stocks and bonds. *Journal of Financial Economics*, 1993.

E. F. Fama and J. D. MacBeth. Risk, return, and equilibrium: Empirical tests. *Journal of political economy*, 81(3):607–636, 1973.

W. E. Ferson and C. R. Harvey. The variation of economic risk premiums. *Journal of Political Economy*, 99(2):385–415, 1991.

W. E. Ferson, S. Kandel, and R. F. Stambaugh. Tests of asset pricing with time-varying expected risk premiums and market betas. *The Journal of Finance*, 42(2):201–220, 1987.

P. Gagliardini, E. Ossola, and O. Scaillet. Time-varying risk premium in large cross-sectional equity data sets. *Econometrica*, 84(3):985–1046, 2016.

E. Ghysels. On stable factor structures in the pricing of risk: do time-varying betas help or hurt? *The Journal of Finance*, 53(2):549–573, 1998.

M. Görgen, A. Jacob, M. Nerlinger, R. Riordan, M. Rohleder, and M. Wilkens. Carbon risk. *Available at SSRN 2930897*, 2019.

S. Grassi and F. Violante. Asset Pricing Using Block-Cholesky GARCH and Time-Varying Betas. Working Papers 2021-05, Center for Research in Economics and Statistics, 2021.

B. E. Hansen. Inference when a nuisance parameter is not identified under the null hypothesis. *Econometrica*, pages 413–430, 1996.

I. Henriques and P. Sadorsky. Oil prices and the stock prices of alternative energy companies. *Energy Economics*, 30(3):998–1010, 2008.

A. Hoepner, P. Masoni, B. Kramer, and et al. Handbook of climate transition benchmarks, paris-aligned benchmark and benchmarks' esg disclosure. Technical report, European Commission, 2019.

T. Jeantheau. Strong consistency of estimators for multivariate arch models. *Econometric theory*, pages 70–86, 1998.

A. Kempf and P. Osthoff. The effect of socially responsible investing on portfolio performance. *European Financial Management*, 13(5):908–922, 2007.

G. Koop, M. H. Pesaran, and S. M. Potter. Impulse response analysis in nonlinear multivariate models. *Journal of econometrics*, 74(1):119–147, 1996.

P. Krueger, Z. Sautner, and L. T. Starks. The importance of climate risks for institutional investors. *The Review of Financial Studies*, 33(3):1067–1111, 2020.

J. Lewellen and S. Nagel. The conditional capm does not explain asset-pricing anomalies. *Journal of financial economics*, 82(2):289–314, 2006.

A. W. Lo and J. Wang. Trading volume: Implications of an intertemporal capital asset pricing model. *The Journal of Finance*, 61(6):2805–2840, 2006.

C. Nobletz et al. Return spillovers between green energy indexes and financial markets: a first sectoral approach. Technical report, University of Paris Nanterre, EconomiX, 2021.

L. Pástor, R. F. Stambaugh, and L. A. Taylor. Sustainable investing in equilibrium. *Journal of Financial Economics*, 2020.

L. Pastor, R. F. Stambaugh, and L. A. Taylor. Dissecting green returns. Technical report, National Bureau of Economic Research, 2021.

Z. Sautner, L. van Lent, G. Vilkov, and R. Zhang. Pricing climate change exposure. *Available at SSRN 3792366*, 2021.

M. Statman. Socially responsible indexes. *The Journal of Portfolio Management*, 32(3): 100–109, 2006.

TCFD. Implementing the recommendations of the task force on climate- related financial disclosure. Technical report, TCFD, 2017.

Appendix A Details on GMB candidates

This section presents details on Green and Brown portfolios formed on different criteria presented in Section 2. Reported average returns and Standard deviations are annualised.

	Mkt share (*100)	Price to Book
Average	2.08	1.30
carbon_TruCost_BinC (GMB1)	0.65	1.02
carbon_TruCost_HS_BinU (GMB2)	0.39	1.31
envScore_ISS_BinU (GMB3)	4.75	1.59
envScore_ISS_BinC	6.84	1.42
carbon_Carbone4_IS_BinU (GMB4)	0.61	0.88
carbon_Carbone4_IS_BinC	0.56	1.03

Table 3: Median values for GMB candidates

	Mean	Sd	Skw	Kurt	Sharpe	emitted	saved	envScore
carbon_TruCost_BinC_Brown (GMB1 Short)	0.084	0.564	-0.717	1.993	0.16	828.46	11.78	2.85
carbon_TruCost_BinC_Green (GMB1 Long)	0.096	0.48	-0.482	1.809	0.2	117.57	6.5	2.91
carbon_TruCost_HS_BinU_Brown (GMB2 Short)	0.084	0.552	-0.545	1.345	0.153	1848.25	18.1	1.9
carbon_TruCost_HS_BinU_Green (GMB2 Long)	0.108	0.6	-0.433	1.672	0.172	305.06	3.59	2.88
envScore_ISS_BinU_Brown (GMB3 Short)	0.084	0.6	-0.486	2.284	0.139	1276.66	11.54	1.26
envScore_ISS_BinU_Green (GMB3 Long)	0.084	0.504	-0.495	0.62	0.165	283.5	10.5	6.75
envScore_ISS_BinC_Brown	0.084	0.588	-0.39	2.308	0.133	967.39	7.39	1.56
envScore_ISS_BinC_Brown	0.084	0.54	-0.494	0.791	0.157	241.45	5.37	6.54
carbon_Carbone4_IS_BinU_Brown (GMB4 Short)	0.06	0.492	-0.498	0.95	0.132	570.56	2.72	3.94
carbon_Carbone4_IS_BinU_Green (GMB4 Long)	0.12	0.588	-0.579	1.575	0.21	265.16	15.22	4.66
carbon_Carbone4_IS_BinC_Brown	0.06	0.564	-0.538	1.304	0.112	399.63	1.91	4.32
carbon_Carbone4_IS_BinC_Green	0.108	0.492	-0.769	2.113	0.225	534.28	21.95	4.42
MKT	0.068	0.547	-0.515	0.959	0.1247			
SMB	0.030	0.372	0.395	5.417	0.082			
HML	0.014	0.398	0.212	3.525	0.035			
GMB1	0.002	0.226	0.156	0.797	0.011			
GMB2	0.014	0.401	0.040	2.228	0.035			
GMB3	-0.008	0.474	0.107	1.861	-0.017			
GMB4	0.058	0.277	0.180	4.236	0.209			

Table 4: Factors statistics

Appendix B Risk premium and conditional betas

This section gives details about conditional regressions outputs.

	Intercept	MKT	SMB	HML	GMB
Coal	-0.13	1.20	0.93	0.66	-0.78
Steel	-0.13	1.38	0.66	0.47	-0.51
Mines	0.01	1.26	0.39	0.36	-0.47
Mach	0.08	1.20	0.36	0.04	-0.44
Chips	0.04	1.17	0.20	-0.50	-0.36
Fin	0.02	1.24	0.07	0.42	-0.33
Banks	0.03	1.02	-0.05	0.67	-0.31
ElcEq	-0.02	1.11	0.48	0.08	-0.30
FabPr	0.01	1.09	0.89	0.18	-0.29
LabEq	0.06	1.08	0.34	-0.32	-0.25
Agric	0.03	0.74	0.21	0.03	-0.23
Chems	0.00	1.06	0.17	0.13	-0.23
Autos	-0.03	1.29	0.40	0.18	-0.21
Comps	-0.02	1.10	0.18	-0.42	-0.18
Other	0.03	0.90	-0.16	0.30	-0.18
Gold	0.05	0.41	0.36	-0.11	-0.17
Trans	0.07	1.02	0.25	0.21	-0.15
Aero	0.05	1.05	0.03	0.18	-0.13
Ships	0.18	1.03	0.28	0.19	-0.13
Paper	-0.06	0.95	-0.01	0.05	-0.08
BldMt	0.02	1.11	0.42	0.31	-0.08
Rubbr	0.04	0.94	0.39	0.05	-0.07
MedEq	0.09	0.89	0.03	-0.20	-0.06
Drugs	0.05	0.83	-0.14	-0.42	-0.06
Oil	-0.08	1.02	0.01	0.53	-0.04
BusSv	0.02	1.09	0.03	-0.44	0.01
Cnstr	0.03	1.24	0.63	0.43	0.05
PerSv	0.01	0.93	0.41	0.19	0.06
RlEst	0.02	1.00	0.42	0.31	0.07
Boxes	0.12	0.99	0.12	0.13	0.10
Insur	0.06	1.00	-0.09	0.42	0.10
Guns	0.20	0.65	-0.16	0.00	0.12
Fun	0.16	1.25	0.20	0.00	0.14
Toys	-0.03	0.94	0.45	0.15	0.15
Food	0.06	0.60	-0.16	-0.04	0.16
Hshld	0.08	0.62	-0.22	-0.07	0.18
Whlsl	0.02	0.96	0.26	0.09	0.19
Txtls	0.06	1.16	0.46	0.32	0.20
Hlth	0.05	0.82	0.23	0.07	0.22
Smoke	0.14	0.69	-0.18	0.14	0.25
Util	0.10	0.69	-0.26	0.20	0.28
Books	-0.09	0.94	0.22	0.38	0.30
Meals	0.13	0.83	0.10	0.06	0.32
Beer	0.09	0.64	-0.36	-0.04	0.33
Telcm	-0.01	0.96	-0.18	0.24	0.35
Clths	0.10	1.06	0.28	0.16	0.38
Soda	0.08	0.84	-0.28	0.02	0.43
Rtail	0.03	1.00	0.01	0.05	0.88

Table 5: Average factor loadings from ACB regressions / Model GMB1

MKT		Model ACB			
		GMB1	GMB2	GMB3	GMB4
Model Rolling	GMB1	0.98	0.97	0.97	0.97
	GMB2	0.98	0.98	0.98	0.98
	GMB3	0.98	0.98	0.98	0.97
	GMB4	0.97	0.98	0.96	0.99

Table 6: MKT Beta rankings correlation between models

SMB		Model ACB			
		GMB1	GMB2	GMB3	GMB4
Model Rolling	GMB1	0.98	0.96	0.96	0.95
	GMB2	0.96	0.97	0.93	0.96
	GMB3	0.97	0.93	0.98	0.93
	GMB4	0.96	0.97	0.93	0.97

Table 7: SMB Beta rankings correlation between models

HML		Model ACB			
		GMB1	GMB2	GMB3	GMB4
Model Rolling	GMB1	0.90	0.80	0.69	0.81
	GMB2	0.94	0.95	0.84	0.95
	GMB3	0.85	0.84	0.93	0.83
	GMB4	0.89	0.90	0.73	0.92

Table 8: HML Beta rankings correlation between models

GMB		Model ACB			
		GMB1	GMB2	GMB3	GMB4
Model Rolling	GMB1	0.98	0.13	0.34	-0.12
	GMB2	0.01	0.92	0.63	0.67
	GMB3	0.31	0.57	0.97	0.29
	GMB4	-0.18	0.52	0.26	0.95

Table 9: GMB Beta rankings correlation between models

	GMB1	GMB2	GMB3	GMB4
Agric	1.80	1.1	2.9	5.3
Food	5.50	1.5	0.9	1.2
Soda	1.40	1.9	0.7	1.0
Beer	2.50	1.4	1.2	1.4
Smoke	2.50	1.3	1.0	9.7
Toys	1.50	1.0	4.3	1.1
Fun	1.10	4.5	0.8	6.7
Books	0.50	2.7	4.8	2.6
Hshld	0.60	0.6	1.0	1.7
Clths	1.70	4.9	1.3	4.9
Hlth	0.50	4.0	2.1	1.0
MedEq	0.90	0.5	1.6	3.4
Drugs	3.40	2.9	2.0	3.5
Chems	2.3	1.9	0.9	1.2
Rubbr	1.70	3.1	0.7	2.2
Txtls	0.80	2.5	1.2	1.3
BldMt	1.20	1.0	1.4	3.3
Cnstr	1.40	2.4	0.9	1.3
Steel	1.60	2.7	1.2	1.8
FabPr	0.60	1.0	0.9	0.7
Mach	1.80	2.1	1.2	8.5
ElcEq	1.60	1.1	1.0	4.6
Autos	0.90	1.9	1.3	2.0
Aero	0.40	2.1	1.2	4.5
Ships	4.80	1.7	0.7	10.8
Guns	2.3	6.0	1.1	0.8
Gold	1.00	1.9	1.3	3.3
Mines	1.20	1.4	1.2	4.2
Coal	1.40	6.6	2.6	1.1
Oil	1.40	1.0	0.9	1.4
Util	1.90	1.1	1.4	5.9
Telcm	1.70	2.5	1.9	2.7
PerSv	1.50	2.6	1.1	2.1
BusSv	2.10	1.4	2.4	1.2
Comps	2.3	1.3	0.9	2.6
Chips	1.00	3.5	1.2	3.3
LabEq	2.00	1.4	2.9	1.3
Paper	2.00	2.1	1.2	0.9
Boxes	2.60	2.1	0.7	0.6
Trans	1.60	2.3	2.0	9.4
Whlsl	1.20	0.9	0.9	1.3
Rtail	0.80	1.0	1.2	2.1
Meals	4.00	7.0	0.9	1.5
Banks	1.00	1.6	1.6	0.9
Insur	0.90	1.1	1.8	0.9
RlEst	1.00	11.8	1.0	1.8
Fin	1.40	0.9	1.3	0.7
Other	5.50	2.0	3.5	2.1

Table 10: Factor loadings volatility ratios between rolling windows regressions and ACB regressions

	Fama-MacBeth				Conditional Risk Premium			
GMB1	-4.83				2.59***			
	(10.34)				(0.50)			
GMB2		21.56*				4.12***		
		(12.98)				(1.48)		
GMB3			10.05				-0.26	
			(13.05)				(0.33)	
GMB4				11.45				1.35***
				(9.98)				(0.61)
MKT	23.81	17.67	18.66	9.79	4.11***	3.86***	3.78***	4.28***
	(18.55)	(18.29)	(17.84)	(17.67)	(0.16)	(0.18)	(0.15)	(0.15)
SMB	-2.46	-6.65	4.36	-2.64	-1.86***	-4.06***	-1.47***	-3.9***
	(10.2)	(10.7)	(10.17)	(10.62)	(0.47)	(1.04)	(0.40)	(0.76)
HML	-12.42	-12.33	-11.61	-9.05	-1.35	-0.64	-2.02***	-3.06***
	(11.28)	(11.12)	(4.15)	(10.28)	(0.51)	(0.44)	(0.34)	(0.46)

$^{***}p < 0.01$, $^{**}p < 0.05$, $^{*}p < 0.1$

Table 11: Factors average risk premium

Appendix C Updating equations of the Score-Driven conditional regression coefficients

This appendix presents the main idea of Score-Driven models and how it is applied to the conditional regression to derive the updating equations presented in (4).

Score Driven models, also known as Generalized Autoregressive Score models (GAS) were introduced by Creal et al. [2013]. They aim at generalizing models with time-varying parameters where the updating is *observation driven*. In particular, consider an observable process y_t and assume it follows the conditional density $p(y_t|\psi_t, \Omega_t, \theta)$ where ψ_t is the time varying parameter of interest, θ a constant parameter, and Ω_t the information set available at time t. A Score Driven models features an updating equation of the form

$$\psi_{t+1} = \overline{\omega} + \xi \underbrace{S(\psi_t) \frac{\partial \log p(y_t|\psi_t, \Omega_t, \theta)}{\partial \psi_t}}_{\text{updating term}} + c\ \psi_t \tag{8}$$

where $\overline{\omega}$, ξ and c are unknown parameters to be estimated. The updating term is decomposed into a scaling term $S(\psi_t)$, that is usually related to the inverse of the information matrix, and the score of the likelihood with respect of the time-varying parameter. The dynamics of the parameter of interest is thus driven by the scaled score. Interestingly, numerous econometric models can be expressed as a Score-Driven model. For example, if we assume that the observation conditional density is Gaussian and the parameter of interest is the time-varying variance, under an appropriate choice of the scaling function, Equation (8) yields the standard GARCH(1,1) model.

Blasques et al. [2022] built on this idea to derive a Score-Driven updating of the conditional regression parameters. If we assume for all i, $\varepsilon_{i,t} = g_{i,t}\nu_{i,t}$ where $\nu_{i,t}$ are iid Gaussian, we obtain the log-likelihood contribution at time t

$$l_{i,t} = \frac{\varepsilon_{i,t}^2}{g_{i,t}^2} + \log(g_{i,t}^2), \quad \varepsilon_{i,t} = r_{i,t} - \sum_{j=1}^{m} \beta_{i,j,t} f_{j,t}. \tag{9}$$

We thus obtain that

$$\frac{\partial l_{i,t}}{\partial \beta_{i,j,t}} = -\frac{2\varepsilon_{i,t} f_{j,t}}{g_{i,t}^2}$$

and the inverse of the information matrix is

$$S(\beta_{i,j,t}) = -\left(\mathbb{E}\left[\frac{\partial^2 l_{i,t}}{\partial \beta_{i,j,t}^2} | \mathcal{F}_{t-1}\right]\right)^{-1} = -\frac{g_{i,t}^2}{2(\mu_j^2 + \sigma_{j,t}^2)}.$$

Whence, we obtain the updating term

$$S(\beta_{i,j,t}) \frac{\partial l_{i,t}}{\partial \beta_{i,j,t}} = \frac{\varepsilon_{i,t} f_{j,t}}{(\mu_j^2 + \sigma_{j,t}^2)}$$

which yields the updating equations in (4).

Appendix D Inference and Hypothesis testing in the ACB model

This section presents the asymptotic results established by Blasques et al. [2022] on the consistency and asymptotic normality of the multistep QML estimator. Building upon these results, we present a test procedure to verify beta constancy and significance. In particular, we establish the asymptotic distribution of the Wald, Quasi Likelihood ratio, and Rao-score test statistics.

D.1 Asymptotics of the multistep QML estimator

Let us denote for any $j \in \{1, \dots, m\}$ the true parameter $\boldsymbol{\theta}_0^{(j)} = (\mu_{0j}, \omega_{0j}, a_{0j}, b_{0j})'$ driving the individual GARCH(1,1) equations of each factor f_j as defined in (2). The first step of the estimation consists of estimating independently $\boldsymbol{\theta}_0^{(j)}$ by standard QML

$$\widehat{\boldsymbol{\theta}}_n^{(j)} = \underset{\boldsymbol{\theta}\in\Theta}{\arg\min}\ \tilde{O}_n^{(j)}(\boldsymbol{\theta}), \qquad \tilde{O}_n^{(j)}(\boldsymbol{\theta}) = \frac{1}{n}\sum_{t=2}^{n} \tilde{l}_{jt}(\boldsymbol{\theta}) \tag{10}$$

where $\boldsymbol{\theta}$ is a generic element of the parameter space Θ and

$$\tilde{l}_{jt}(\boldsymbol{\theta}) = \frac{(f_{j,t}-\mu)^2}{\tilde{\sigma}_{j,t}^2(\boldsymbol{\theta})} + \log \tilde{\sigma}_{j,t}^2(\boldsymbol{\theta}), \quad \tilde{\sigma}_{j,t}^2(\boldsymbol{\theta}) = \omega + a(f_{j,t-1}-\mu)^2 + b\tilde{\sigma}_{j,t-1}^2(\boldsymbol{\theta})$$

with a given initial value $\tilde{\sigma}_{j,1}^2(\boldsymbol{\theta}) = \tilde{g} > 0$.

In the second step, we estimate the parameter driving the GARCH(1,1) equation (3) of the residuals $\varepsilon_{i,t}$ denoted $\boldsymbol{\vartheta}_0^{(\varepsilon_i)} = (\omega_{0\varepsilon_i}, a_{0\varepsilon_i}, b_{0\varepsilon_i})'$, the parameter $\boldsymbol{\vartheta}_0^{(i,0)} = (\overline{\omega}_{0\alpha_i}, \xi_{0\alpha_i}, c_{0\alpha_i})'$ driving the dynamic of the time-varying intercept, and $\boldsymbol{\vartheta}_0^{(i,j)} = (\overline{\omega}_{0,i,j}, \xi_{0,i,j}, c_{0,i,j})'$ the parameter driving the dynamic of the time-varying $\beta_{i,j}$, for $j \in \{1, \dots, m\}$. Let $\boldsymbol{\vartheta}_0^{(i)} = (\boldsymbol{\vartheta}_0^{(\varepsilon_i)'}, \boldsymbol{\vartheta}_0^{(i,0)'}, \boldsymbol{\vartheta}_0^{(i,1)'}, \dots, \boldsymbol{\vartheta}_0^{(i,m)'})'$, $\boldsymbol{\theta}_0 = (\boldsymbol{\theta}_0^{(1)'}, \dots, \boldsymbol{\theta}_0^{(m)'})'$ and the full parameter $\boldsymbol{\varphi}_0^{(i)} = (\boldsymbol{\theta}_0', \boldsymbol{\vartheta}_0^{(i)'})'$. Let $\boldsymbol{\vartheta}$ a generic element of $\Theta_{\boldsymbol{\vartheta}}$ and $\boldsymbol{\varphi} = (\boldsymbol{\theta}', \boldsymbol{\vartheta}')'$. We estimate $\boldsymbol{\vartheta}_0^{(i)}$ by

$$\widehat{\boldsymbol{\vartheta}}_n^{(i)} = \underset{\boldsymbol{\vartheta}\in\Theta_{\boldsymbol{\vartheta}}}{\arg\min}\ \tilde{O}_n(\widehat{\boldsymbol{\theta}}_n, \boldsymbol{\vartheta}), \qquad \tilde{O}_n^{(i)}(\boldsymbol{\varphi}) = \frac{1}{n}\sum_{t=2}^{n} \tilde{l}_t^{(i)}(\boldsymbol{\varphi}) \tag{11}$$

where

$$\begin{aligned}
\tilde{l}_t^{(i)}(\boldsymbol{\varphi}) &= \frac{\tilde{\varepsilon}_{i,t}(\boldsymbol{\varphi})}{\tilde{g}_{i,t}^2(\boldsymbol{\varphi})} + \log \tilde{g}_{i,t}^2(\boldsymbol{\varphi}), \quad \tilde{\varepsilon}_{i,t}(\boldsymbol{\varphi}) = r_{i,t} - \tilde{\alpha}_{i,t}(\boldsymbol{\varphi}) - \sum_{j=1}^{m} \tilde{\beta}_{i,j,t}(\boldsymbol{\varphi}) f_{j,t}, \\
\tilde{g}_{i,t}^2(\boldsymbol{\varphi}) &= \omega + \alpha \tilde{v}_{i,t-1}^2(\boldsymbol{\varphi}) + \beta \tilde{g}_{i,t-1}^2(\boldsymbol{\varphi}), \quad \tilde{\alpha}_{i,t}(\boldsymbol{\varphi}) = \overline{\omega}_{\alpha_i} + \xi_{\alpha_i} \tilde{\varepsilon}_{i,t-1}(\boldsymbol{\varphi}) + c_{\alpha_i} \tilde{\alpha}_{i,t-1}(\boldsymbol{\varphi}) \\
\tilde{\beta}_{i,j,t}(\boldsymbol{\varphi}) &= \overline{\omega}_{i,j} + \xi_{i,j} \frac{f_{j,t-1}\ \tilde{\varepsilon}_{i,t-1}(\boldsymbol{\varphi})}{\mu_j^2 + \tilde{\sigma}_{j,t-1}^2(\boldsymbol{\theta})} + c_{i,j} \tilde{\beta}_{i,j,t-1}(\boldsymbol{\varphi}).
\end{aligned}$$

The multistep QML etimator is thus given by $\widehat{\boldsymbol{\varphi}}_n^{(i)} = (\widehat{\boldsymbol{\theta}}_n', \widehat{\boldsymbol{\vartheta}}_n^{(i)\prime})'$.

Under a set of technical assumptions that we denote **[A-ACB]**, Blasques et al. [2022] show the following results.

Theorem 1 (CAN of the QMLE (Darolles, Francq and Laurent, 2018))**.** *Under the set of assumptions **[A-ACB]**, we have*

$$\widehat{\boldsymbol{\theta}}_n \to \boldsymbol{\theta}_0 \ a.s. \quad \text{and} \quad \widehat{\boldsymbol{\vartheta}}_n^{(i)} \to \boldsymbol{\vartheta}_0^{(i)} \ a.s. \ as \ n \to \infty.$$

In addition,

$$\sqrt{n}(\widehat{\boldsymbol{\varphi}}_n^{(i)} - \boldsymbol{\varphi}_0^{(i)}) \xrightarrow{\mathcal{L}} \mathcal{N}(\mathbf{0}, \boldsymbol{\Omega}_i) \tag{12}$$

where $\boldsymbol{\Omega}_i$ is an invertible matrix.

D.2 Testing for constant conditional betas

Although the assumption of beta constancy is rarely backed by an economic rationale, linear regressions with constant slope parameters remain predominant in the financial literature. It is therefore useful to introduce test procedures to verify this assumption. Moreover, this general testing setup can easily be extended for model selection to assess new factors' relevancy.

Assume that we want to test the hypothesis $H_{0,ij} : \beta_{i,j,t} = \overline{\omega}_{0,ij}$ against $H_{1,ij} : \beta_{i,j,t}$ is time-varying. From (4), constancy of $\beta_{i,j,t}$ is obtained when $\xi_{0ij} = 0$. However, testing for this constraint on $\boldsymbol{\vartheta}_0$ is difficult. Indeed, under $H_{0,ij} : \xi_{0ij} = 0$, the conditional beta $\beta_{i,j,t}$ tends to $\overline{\omega}_{ij}/(1 - c_{ij})$ and there exists an infinity of pairs $(\overline{\omega}_{ij}, c_{ij})$ such that $\beta_{i,j,t} = \overline{\omega}_{0,ij}$, resulting in a non identifiable model under the null hypothesis. Testing problems where parameters are not identified under the null induces non standard asymptotic distributions of the classical tests statistics. Hansen [1996] in particular provides a methodology to conduct such tests. To simplify the testing procedures, we rather suppose that the parameter c_{0ij} is known and set at an arbitrary value $\overline{c}_{ij}$. This solves the identification issue and we can now test $H_{0,ij}(\overline{c}_{ij}) : \xi_{0ij} = 0$ using standard techniques. Let us denote $\boldsymbol{R}$ the constraint matrix such that $\boldsymbol{R}\boldsymbol{\varphi}_0^{(i)} = \xi_{0ij}$. The triptych of the Wald, Rao-score, and Quasi Likelihood Ratio (LR) statistics is given by

$$\begin{aligned}
W_n &= n(\boldsymbol{R}\ \widehat{\boldsymbol{\varphi}}_n^{(i)})' \left(\boldsymbol{R}\widehat{\boldsymbol{\Omega}}_{i,n}\boldsymbol{R}'\right)^{-1} (\boldsymbol{R}\ \widehat{\boldsymbol{\varphi}}_n^{(i)}) \\
R_n &= n\frac{\partial \tilde{O}_n(\widehat{\boldsymbol{\varphi}}_{n|H_{0,ij}}^{(i)})}{\partial \boldsymbol{\varphi}'} \boldsymbol{J}_{n|H_{0,ij}}^{-1} \boldsymbol{R}'(\boldsymbol{R}\widehat{\boldsymbol{\Omega}}_{i,n|H_{0,ij}}\boldsymbol{R}')^{-1}\boldsymbol{R}\boldsymbol{J}_{n|H_{0,ij}}^{-1} \frac{\partial \tilde{O}_n(\widehat{\boldsymbol{\varphi}}_{n|H_{0,ij}}^{(i)})}{\partial \boldsymbol{\varphi}} \\
L_n &= 2n\left[\tilde{O}_n(\widehat{\boldsymbol{\varphi}}_{n|H_{0,ij}}^{(i)}) - \tilde{O}_n(\widehat{\boldsymbol{\varphi}}_n^{(i)})\right]
\end{aligned} \tag{13}$$

where $\widehat{\boldsymbol{\varphi}}^{(i)}_{n|H_{0,ij}}$ is the multistep QMLE restricted by $H_{0,ij}(\overline{c}_{ij})$, $\widehat{\boldsymbol{\Omega}}_{i,n}$ is a consistent estimator of $\boldsymbol{\Omega}_i$, $\widehat{\boldsymbol{\Omega}}_{i,n|H_{0,ij}}$ is a consistent estimator of $\boldsymbol{\Omega}_i$ under $H_{0,ij}(\overline{c}_{ij})$, and

$$\boldsymbol{J}_{n|H_{0,ij}} = \frac{\partial^2 \tilde{O}_n(\widehat{\boldsymbol{\varphi}}^{(i)}_{n|H_{0,ij}})}{\partial\boldsymbol{\varphi}\partial\boldsymbol{\varphi}'}$$

is a consistent estimators of $\boldsymbol{J_i} = \mathbb{E}\dfrac{\partial^2 l_t^{(i)}(\boldsymbol{\varphi}_0)}{\partial\boldsymbol{\varphi}\partial\boldsymbol{\varphi}'}$ under $H_{0,ij}(\overline{c}_{ij})$.

Proposition 1. *Under the set of assumptions* ***[A-ACB]****, under $H_{0,ij}(\overline{c}_{ij})$, W_n and R_n test statistics follow a χ^2_1 distribution and the critical regions at the asymptotic level ν are given by*

$$\left\{W_n > \chi^2_1(1-\nu)\right\}, \left\{R_n > \chi^2_1(1-\nu)\right\}.$$

where $\chi^2_1(1-\nu)$ is the $(1-\nu)$-quantile of the χ^2 distribution with 1 degree of freedom. In addition, under the same assumptions,

$$L_n \to \overline{\chi}(\boldsymbol{\pi}) \text{ with } \overline{\chi}(\boldsymbol{\pi}) = \sum_{j=1}^{7m+3} \pi_i \chi^2_i$$

where $\boldsymbol{\pi} = (\pi_i)_{i=1,\ldots,7m+3}$ is the vector of eigenvalues of the matrix $\boldsymbol{J}^{-1}\boldsymbol{R}'\boldsymbol{\Lambda}\boldsymbol{R}$ with

$$\boldsymbol{\Lambda} = \left[\boldsymbol{R}\boldsymbol{J}^{-1}\boldsymbol{R}'\right]^{-1}\left[\boldsymbol{R}\boldsymbol{\Omega}\boldsymbol{R}'\right]\left[\boldsymbol{R}\boldsymbol{J}^{-1}\boldsymbol{R}'\right]^{-1'}.$$

Proof. We begin by studying the asymptotic distribution of the Wald statistic under the null $H_{0,ij}(\overline{c}_{ij}) : \boldsymbol{R}\boldsymbol{\varphi}^{(i)}_0 = 0$. From (12) and Slutsky lemma, we obtain

$$\sqrt{n}(\boldsymbol{R}\widehat{\boldsymbol{\varphi}}^{(i)}_n - \boldsymbol{R}\boldsymbol{\varphi}^{(i)}_0) = \sqrt{n}\boldsymbol{R}(\widehat{\boldsymbol{\varphi}}^{(i)}_n - \boldsymbol{\varphi}^{(i)}_0) \xrightarrow{\mathcal{L}} \mathcal{N}(\boldsymbol{0}, \boldsymbol{R}\boldsymbol{\Omega}_i\boldsymbol{R}') \tag{14}$$

and from the quadratic form, we thus have

$$n(\boldsymbol{R}\ \widehat{\boldsymbol{\varphi}}^{(i)}_n)'\left(\boldsymbol{R}\widehat{\boldsymbol{\Omega}}_{i,n}\boldsymbol{R}'\right)^{-1}(\boldsymbol{R}\ \widehat{\boldsymbol{\varphi}}^{(i)}_n) \xrightarrow{\mathcal{L}} \chi^2_1$$

under $H_{0,ij}(\overline{c}_{ij}) : \boldsymbol{R}\boldsymbol{\varphi}^{(i)}_0 = 0$. Thus, the critical region of the Wald test at the asymptotic level α is $\left\{W_n > \chi^2_1(1-\alpha)\right\}$.

To study the Rao-score statistic, we first introduce the Lagrangian function associated with the likelihood optimization problem constrained by $H_{0,ij}(\overline{c}_{ij})$, $\tilde{O}_n(\boldsymbol{\varphi}) + (\boldsymbol{R}\boldsymbol{\varphi})'\boldsymbol{\lambda}$. The first-order condition is then

$$\frac{\partial\tilde{O}_n(\widehat{\boldsymbol{\varphi}}^{(i)}_{n|H_{0,ij}})}{\partial\boldsymbol{\varphi}} + \boldsymbol{R}'\tilde{\boldsymbol{\lambda}}_n = 0 \tag{15}$$

with $\tilde{\boldsymbol{\lambda}}_n$ the Lagrange multipliers vector.

Under $H_{0,ij}(\bar{c}_{ij})$, we have

$$\sqrt{n}(\boldsymbol{R}\widehat{\boldsymbol{\varphi}}_n^{(i)}) = \boldsymbol{R}\sqrt{n}(\widehat{\boldsymbol{\varphi}}_n^{(i)} - \boldsymbol{\varphi}_0^{(i)})$$

and

$$0 = \sqrt{n}(\boldsymbol{R}\widehat{\boldsymbol{\varphi}}_{n|H_{0,ij}}^{(i)}) = \boldsymbol{R}\sqrt{n}(\widehat{\boldsymbol{\varphi}}_{n|H_{0,ij}}^{(i)} - \boldsymbol{\varphi}_0^{(i)})$$

since $\widehat{\boldsymbol{\varphi}}_{n|H_{0,ij}}^{(i)}$ is the constrained estimator. By subtraction, we thus obtain

$$\sqrt{n}(\boldsymbol{R}\widehat{\boldsymbol{\varphi}}_n^{(i)}) = \boldsymbol{R}\sqrt{n}(\widehat{\boldsymbol{\varphi}}_n^{(i)} - \widehat{\boldsymbol{\varphi}}_{n|H_{0,ij}}^{(i)}). \tag{16}$$

Using Taylor expansions, we can also notice that

$$0 = \sqrt{n}\frac{\partial \tilde{O}_n(\widehat{\boldsymbol{\varphi}}_n^{(i)})}{\partial \boldsymbol{\varphi}} \overset{o_P(1)}{=} \sqrt{n}\frac{\partial \tilde{O}_n(\boldsymbol{\varphi}_0^{(i)})}{\partial \boldsymbol{\varphi}} + \sqrt{n}\boldsymbol{J}(\widehat{\boldsymbol{\varphi}}_n^{(i)} - \boldsymbol{\varphi}_0^{(i)}) \tag{17}$$

and

$$\sqrt{n}\frac{\partial \tilde{O}_n(\widehat{\boldsymbol{\varphi}}_{n|H_{0,ij}}^{(i)})}{\partial \boldsymbol{\varphi}} \overset{o_P(1)}{=} \sqrt{n}\frac{\partial \tilde{O}_n(\boldsymbol{\varphi}_0^{(i)})}{\partial \boldsymbol{\varphi}} + \sqrt{n}\boldsymbol{J}(\widehat{\boldsymbol{\varphi}}_{n|H_{0,ij}}^{(i)} - \boldsymbol{\varphi}_0^{(i)})$$

which yields by subtraction

$$\sqrt{n}\frac{\partial \tilde{O}_n(\widehat{\boldsymbol{\varphi}}_{n|H_{0,ij}}^{(i)})}{\partial \boldsymbol{\varphi}} \overset{o_P(1)}{=} -\sqrt{n}\boldsymbol{J}(\widehat{\boldsymbol{\varphi}}_n^{(i)} - \widehat{\boldsymbol{\varphi}}_{n|H_{0,ij}}^{(i)})$$

hence

$$\sqrt{n}(\widehat{\boldsymbol{\varphi}}_n^{(i)} - \widehat{\boldsymbol{\varphi}}_{n|H_{0,ij}}^{(i)}) \overset{o_P(1)}{=} -\sqrt{n}\boldsymbol{J}^{-1}\frac{\partial \tilde{O}_n(\widehat{\boldsymbol{\varphi}}_{n|H_{0,ij}}^{(i)})}{\partial \boldsymbol{\varphi}}. \tag{18}$$

From (15), (16) and (18), we thus obtain

$$\sqrt{n}(\boldsymbol{R}\tilde{\boldsymbol{\vartheta}}_n) \overset{o_P(1)}{=} \boldsymbol{R}\boldsymbol{J}^{-1}\boldsymbol{R}'\sqrt{n}\tilde{\boldsymbol{\lambda}}_n \tag{19}$$

which yields

$$\sqrt{n}\tilde{\boldsymbol{\lambda}}_n \overset{o_P(1)}{=} \left[\boldsymbol{R}\boldsymbol{J}^{-1}\boldsymbol{R}'\right]^{-1}\sqrt{n}(\boldsymbol{R}\widehat{\boldsymbol{\varphi}}_n^{(i)})$$

hence from (14), under $H_{0,ij}(\bar{c}_{ij})$,

$$\sqrt{n}\tilde{\boldsymbol{\lambda}}_n \xrightarrow{\mathcal{L}} \mathcal{N}(\boldsymbol{0}, \boldsymbol{\Lambda}) \text{ with } \boldsymbol{\Lambda} = \left[\boldsymbol{R}\boldsymbol{J}^{-1}\boldsymbol{R}'\right]^{-1}\left[\boldsymbol{R}\boldsymbol{\Omega}\boldsymbol{R}'\right]\left[\boldsymbol{R}\boldsymbol{J}^{-1}\boldsymbol{R}'\right]^{-1'}$$

as $n \to \infty$. Taking the quadratic form, we obtain under $H_{0,ij}(\overline{c}_{ij})$,

$$n\tilde{\boldsymbol{\lambda}}_n' \boldsymbol{R} \hat{\boldsymbol{J}}_{n|H_{0,ij}}^{-1} \boldsymbol{R}' (\boldsymbol{R} \widehat{\boldsymbol{\Omega}}_{i,n|H_{0,ij}} \boldsymbol{R}')^{-1} \boldsymbol{R} \hat{\boldsymbol{J}}_{n|H_{0,ij}}^{-1} \boldsymbol{R}' \tilde{\boldsymbol{\lambda}}_n \xrightarrow{\mathcal{L}} \chi_1^2$$

and (15) yields

$$n \frac{\partial \tilde{O}_n(\widehat{\boldsymbol{\varphi}}_{n|H_{0,ij}}^{(i)})}{\partial \boldsymbol{\varphi}} \hat{\boldsymbol{J}}_{n|H_{0,ij}}^{-1} \boldsymbol{R}' (\boldsymbol{R} \widehat{\boldsymbol{\Omega}}_{i,n|H_{0,ij}} \boldsymbol{R}')^{-1} \boldsymbol{R} \hat{\boldsymbol{J}}_{n|H_{0,ij}}^{-1} \frac{\partial \tilde{O}_n(\widehat{\boldsymbol{\varphi}}_{n|H_{0,ij}}^{(i)})}{\partial \boldsymbol{\varphi}} \xrightarrow{\mathcal{L}} \chi_1^2. \tag{20}$$

It follows that the critical region of the Rao-score test at the asymptotic level α is $\{R_n > \chi_1^2(1-\alpha)\}$.

We finally focus on the Quasi Likelihood Ratio statistic. Using Taylor expansions, we get

$$\tilde{O}_n(\widehat{\boldsymbol{\varphi}}_n^{(i)}) \overset{o_P(1)}{=} \tilde{O}_n(\boldsymbol{\varphi}_0^{(i)}) + \frac{\partial \tilde{O}_n(\boldsymbol{\varphi}_0^{(i)})}{\partial \boldsymbol{\varphi}'} (\widehat{\boldsymbol{\varphi}}_n^{(i)} - \boldsymbol{\varphi}_0^{(i)}) + \frac{1}{2} (\widehat{\boldsymbol{\varphi}}_n^{(i)} - \boldsymbol{\varphi}_0^{(i)})' \boldsymbol{J} (\widehat{\boldsymbol{\varphi}}_n^{(i)} - \boldsymbol{\varphi}_0^{(i)})$$

and

$$\tilde{O}_n(\widehat{\boldsymbol{\varphi}}_{n|H_{0,ij}}^{(i)}) \overset{o_P(1)}{=} \tilde{O}_n(\boldsymbol{\varphi}_0^{(i)}) + \frac{\partial \tilde{O}_n(\boldsymbol{\varphi}_0^{(i)})}{\partial \boldsymbol{\varphi}'} (\widehat{\boldsymbol{\varphi}}_{n|H_{0,ij}}^{(i)} - \boldsymbol{\varphi}_0^{(i)}) + \frac{1}{2} (\widehat{\boldsymbol{\varphi}}_{n|H_{0,ij}}^{(i)} - \boldsymbol{\varphi}_0^{(i)})' \boldsymbol{J} (\widehat{\boldsymbol{\varphi}}_{n|H_{0,ij}}^{(i)} - \boldsymbol{\varphi}_0^{(i)}),$$

hence, by subtraction,

$$\begin{aligned} L_n \overset{o_P(1)}{=} \; & 2n \frac{\partial \tilde{O}_n(\boldsymbol{\varphi}_0^{(i)})}{\partial \vartheta'} (\widehat{\boldsymbol{\varphi}}_{n|H_{0,ij}}^{(i)} - \widehat{\boldsymbol{\varphi}}_n^{(i)}) + n (\widehat{\boldsymbol{\varphi}}_{n|H_{0,ij}}^{(i)} - \boldsymbol{\varphi}_0^{(i)})' \boldsymbol{J} (\widehat{\boldsymbol{\varphi}}_{n|H_{0,ij}}^{(i)} - \boldsymbol{\varphi}_0^{(i)}) \\ & - n (\widehat{\boldsymbol{\varphi}}_n^{(i)} - \boldsymbol{\varphi}_0^{(i)})' \boldsymbol{J} (\widehat{\boldsymbol{\varphi}}_n^{(i)} - \boldsymbol{\varphi}_0^{(i)}), \end{aligned}$$

and, from (17),

$$\begin{aligned} L_n \overset{o_P(1)}{=} \; & 2n (\widehat{\boldsymbol{\varphi}}_n^{(i)} - \boldsymbol{\varphi}_0^{(i)})' \boldsymbol{J} (\widehat{\boldsymbol{\varphi}}_{n|H_{0,ij}}^{(i)} - \widehat{\boldsymbol{\varphi}}_n^{(i)}) \\ & + n (\widehat{\boldsymbol{\varphi}}_{n|H_{0,ij}}^{(i)} - \boldsymbol{\varphi}_0^{(i)})' \boldsymbol{J} (\widehat{\boldsymbol{\varphi}}_{n|H_{0,ij}}^{(i)} - \boldsymbol{\varphi}_0^{(i)}) - n (\widehat{\boldsymbol{\varphi}}_n^{(i)} - \boldsymbol{\varphi}_0^{(i)})' \boldsymbol{J} (\widehat{\boldsymbol{\varphi}}_n^{(i)} - \boldsymbol{\varphi}_0^{(i)}) \\ \overset{o_P(1)}{=} \; & n (\widehat{\boldsymbol{\varphi}}_n^{(i)} - \widehat{\boldsymbol{\varphi}}_{n|H_{0,ij}}^{(i)})' \boldsymbol{J} (\widehat{\boldsymbol{\varphi}}_n^{(i)} - \widehat{\boldsymbol{\varphi}}_{n|H_{0,ij}}^{(i)}). \end{aligned}$$

From (15) and (18), it follows that under $H_{0,ij}(\overline{c}_{ij})$,

$$L_n \overset{o_P(1)}{=} \sqrt{n} \boldsymbol{R}' \tilde{\boldsymbol{\lambda}}_n \boldsymbol{J}^{-1} \tilde{\boldsymbol{\lambda}}_n' \boldsymbol{R} \sqrt{n} \tag{21}$$

and, from (19), Slutsky lemma, and the quadratic form of multivariate normally dis-

tributed variables, we obtain

$$L_n \to \overline{\chi}(\boldsymbol{\pi}) \text{ with } \overline{\chi}(\boldsymbol{\pi}) = \sum_{i=1}^{7m+3} \pi_i \chi_i^2$$

where $\boldsymbol{\pi} = (\pi_i)_{i=1,\ldots,7m+3}$ is the vector of eigenvalues of the matrix $\boldsymbol{J}^{-1}\boldsymbol{R}'\boldsymbol{\Lambda}\boldsymbol{R}$ with

$$\boldsymbol{\Lambda} = \left[\boldsymbol{R}\boldsymbol{J}^{-1}\boldsymbol{R}'\right]^{-1}\left[\boldsymbol{R}\boldsymbol{\Omega}\boldsymbol{R}'\right]\left[\boldsymbol{R}\boldsymbol{J}^{-1}\boldsymbol{R}'\right]^{-1'}.$$

□

Appendix E Spillover Persistence in the unrestricted ECCC GARCH model

This section builds upon Conrad and Karanasos [2010] and Conrad and Weber [2013] to detail the computation of the $\lambda_{ij,k}$ coefficients.

Let us consider the *univariate* representation of Equation (7). We denote

$$\boldsymbol{A}(L) = \sum_{i=1}^{q} \boldsymbol{A}_i L^i, \quad \text{and} \quad \boldsymbol{B}(L) = \boldsymbol{I}_2 - \sum_{j=1}^{p} \boldsymbol{B}_j L^j,$$

and let $\beta(L) = 1 - \sum_{j=1}^{2\times p} \beta_j L^j = \det \boldsymbol{B}(L)$. We can rewrite (7) as

$$\boldsymbol{B}(L)\boldsymbol{g}_t = \boldsymbol{\omega} + \boldsymbol{A}(L)\boldsymbol{r}_t^2 \Leftrightarrow \beta(L)\boldsymbol{g}_t = \boldsymbol{\mu} + \boldsymbol{\alpha}(L)\boldsymbol{r}_t^2 \tag{22}$$

with $\boldsymbol{\mu} = \text{adj}[\boldsymbol{B}(1)]\boldsymbol{\omega}$ and $\boldsymbol{\alpha}(L) = \text{adj}[\boldsymbol{B}(L)]\boldsymbol{A}(L)$ and thus we obtain the ARCH(∞) form

$$\boldsymbol{g}_t = \boldsymbol{\mu}/\beta(1) + \boldsymbol{\Phi}(L)\boldsymbol{r}_t^2, \tag{23}$$

with $\boldsymbol{\Phi}(L) = [\Phi_{ij}(L)]_{i,j=1,2} = \boldsymbol{\alpha}(L)/\beta(L)$. Note that $\Phi_{ij}(L) = \alpha_{ij}(L)/\beta(L) = \sum_{k=i}^{\infty} \Phi_{ij,k} L^k$ can be thought as the ARCH(∞) kernel of a GARCH($2p, p+q$).

Consider now the UECCC-GARCH(1,1) equation

$$\boldsymbol{g}_t = \boldsymbol{\omega} + \boldsymbol{A}\boldsymbol{r}_{t-1}^2 + \boldsymbol{B}\boldsymbol{g}_{t-1}. \tag{24}$$

Similarly to (23), we obtain the rewriting in term of volatility innovations $\boldsymbol{h}_t$

$$\boldsymbol{C}(L)\boldsymbol{g}_t = \boldsymbol{\omega} + \boldsymbol{A}(L)\boldsymbol{h}_t \Leftrightarrow \gamma(L)\boldsymbol{g}_t = \text{adj}[\boldsymbol{C}(1)]\boldsymbol{\omega} + \text{adj}[\boldsymbol{C}(L)]\boldsymbol{A}(L)\boldsymbol{h}_t$$

where $\boldsymbol{C}(L) = \boldsymbol{I}_2 - \boldsymbol{C}L$, $\boldsymbol{C} = \boldsymbol{A} + \boldsymbol{B}$, $\boldsymbol{A}(L) = \boldsymbol{A}L$, and $\gamma(L) = 1 - \sum_{j=1}^{2p} \gamma_j L^j = \det \boldsymbol{C}(L)$. Thus we can derive the ARCH(∞) representation

$$\boldsymbol{g}_t = \text{adj}[\boldsymbol{C}(1)]\boldsymbol{\omega}/\gamma(1) + \boldsymbol{\Lambda}(L)\boldsymbol{h}_t,$$

with $\boldsymbol{\Lambda}(L) = [\lambda_{ij}(L)]_{i,j=1,2} = \dfrac{\text{adj}[\boldsymbol{C}(L)]\boldsymbol{A}(L)}{\gamma(L)}$. We thus have that the coefficients $\lambda_{ij,k}$

of the ARCH(∞) kernels $[\lambda_{ij}(L)]_{i,j=1,2} = \sum_{k=i}^{\infty} \lambda_{ij,k} L^k$ verify

$$\lambda_{ii,k} = \frac{\partial g_{i,t}}{\partial h_{i,t-k}} \text{ and } \lambda_{ij,k} = \frac{\partial g_{i,t}}{\partial h_{j,t-k}}.$$

As noted by Conrad and Weber [2013], the bivariate uECCC-GARCH(1,1) model allows for a simple recursive expression of the $\lambda_{ij,k}$ coefficients. Indeed, we have the univariate GARCH(2,2) representation in terms of $\boldsymbol{h}_t$ of equation (24)

$$\gamma(L)\boldsymbol{g}_t = \text{adj}[\boldsymbol{C}(1)]\boldsymbol{\omega} + \boldsymbol{\alpha}^{(1)}\boldsymbol{h}_{t-1} + \boldsymbol{\alpha}^{(2)}\boldsymbol{h}_{t-2}$$

where

$$\begin{aligned}
\boldsymbol{\alpha}^{(1)} &= \begin{pmatrix} a_{11} & a_{12} \\ a_{21} & a_{22} \end{pmatrix} \\
\boldsymbol{\alpha}^{(2)} &= \begin{pmatrix} a_{21}(a_{12}+b_{12}) - a_{11}(a_{22}+a_{22}) & a_{22}b_{12} - a_{12}b_{22} \\ a_{11}b_{12} - a_{21}b_{11} & a_{12}(a_{21}+b_{21}) - a_{22}(a_{11}+a_{11}) \end{pmatrix}
\end{aligned}$$

where a_{ij} and b_{ij} are elements of matrices $\boldsymbol{A}$ and $\boldsymbol{B}$ respectively. We can recursively express

$$\lambda_{ij,k} = \gamma_1 \lambda_{ij,k-1} + \gamma_2 \lambda_{ij,k-2}, \quad \text{for } k \leq 3$$

with $\lambda_{ij,1} = \alpha_{ij}^{(1)}$, $\lambda_{ij,2} = \gamma_1 \alpha_{ij}^{(1)} + \alpha_{ij}^{(2)}$ where $\gamma_1 = c_{11} + c_{22}$, $\gamma_2 = c_{12}c_{21} - c_{11}c_{22}$, and c_{ij} are elements of matrix $\boldsymbol{C}$.

Appendix F Green and Brown portfolios formed on other criteria

(a) *Portfolio Tracks*

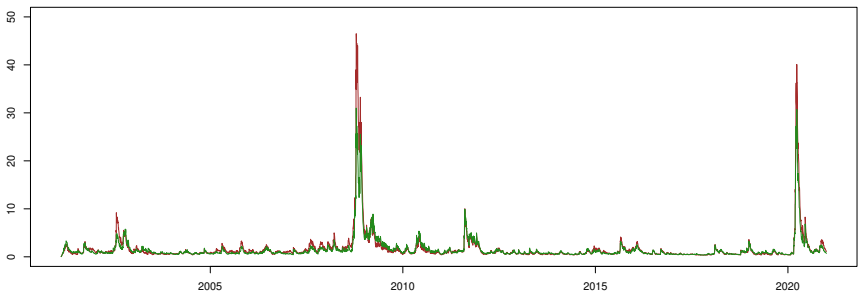

(b) *Conditional volatilities*

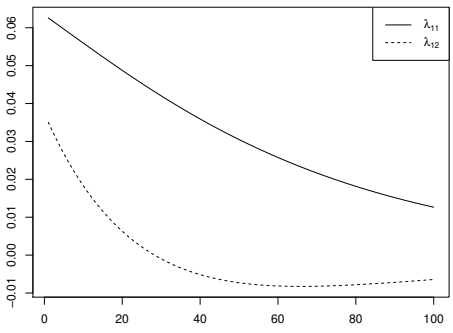

(c) *Response function of* $g_{B,t}$

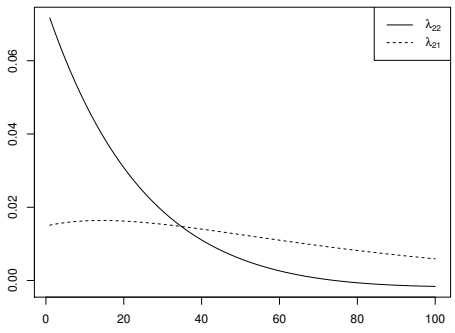

(d) *Response function of* $g_{G,t}$

Figure 10: *Performance, Conditional volatilities, and Response functions of Brown and Green portfolios formed on GMB2 criterion.*

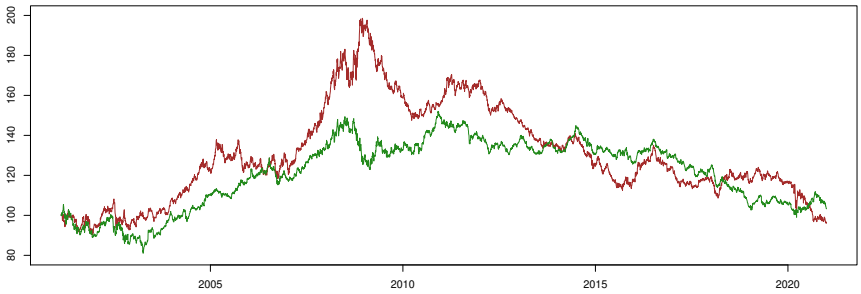

(a) *Portfolio Tracks*

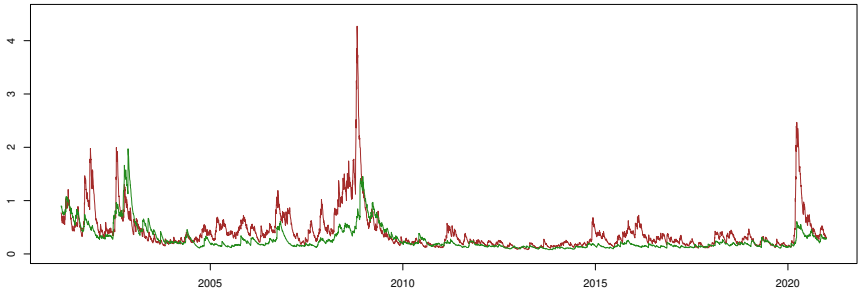

(b) *Conditional volatilities*

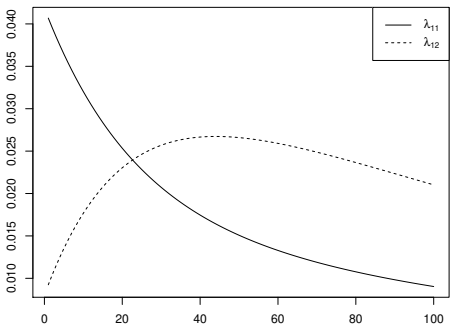

(c) *Response function of* $g_{B,t}$

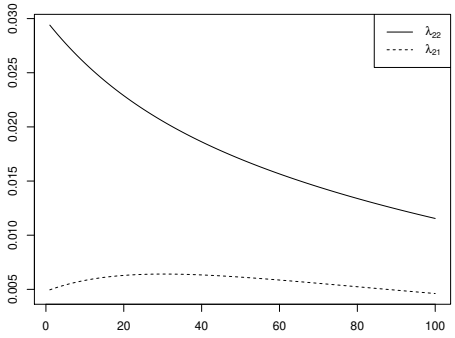

(d) *Response function of* $g_{G,t}$

Figure 11: *Performance, Conditional volatilities, and Response functions of Brown and Green portfolios formed on GMB2 criterion hedged of Fama French factors.*

(a) *Portfolio Tracks*

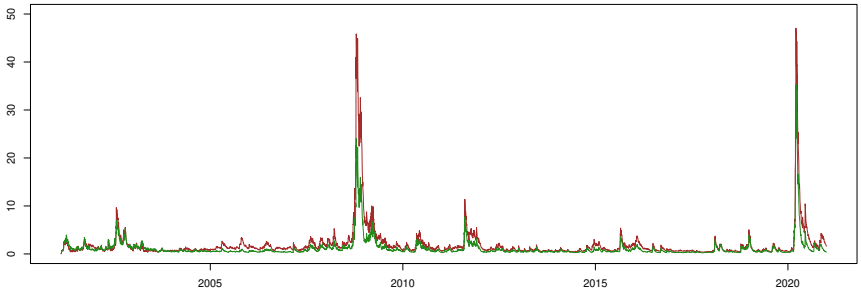

(b) *Conditional volatilities*

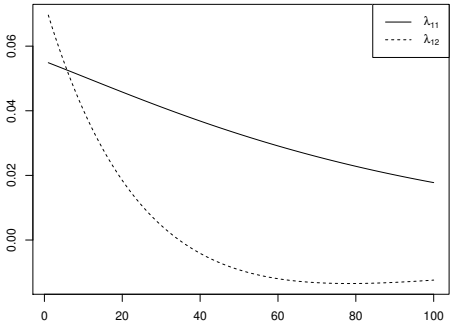

(c) *Response function of* $g_{B,t}$

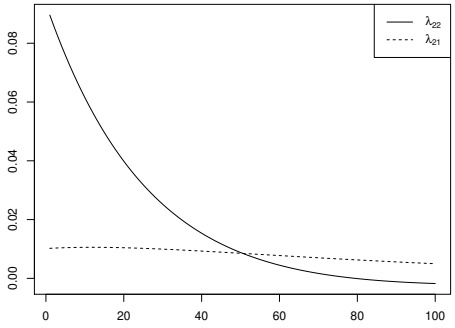

(d) *Response function of* $g_{G,t}$

Figure 12: *Performance, Conditional volatilities, and Response functions of Brown and Green portfolios formed on GMB3 criterion.*

(a) *Portfolio Tracks*

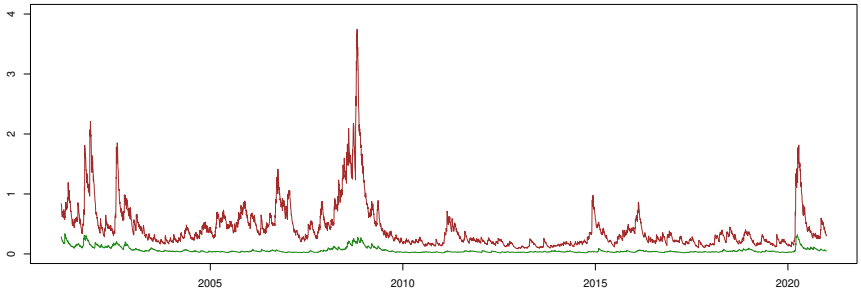

(b) *Conditional volatilities*

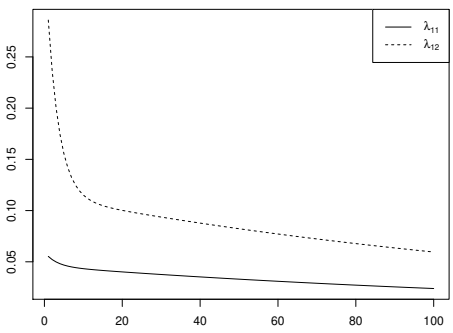

(c) *Response function of* $g_{B,t}$

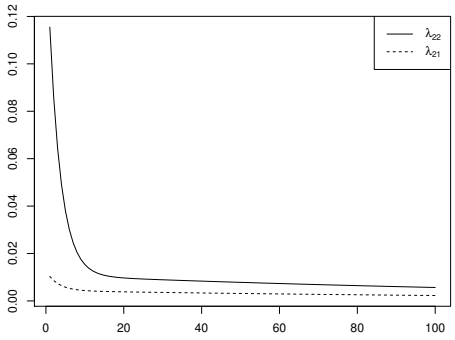

(d) *Response function of* $g_{G,t}$

Figure 13: *Performance, Conditional volatilities, and Response functions of Brown and Green portfolios formed on GMB3 criterion hedged of Fama French factors.*

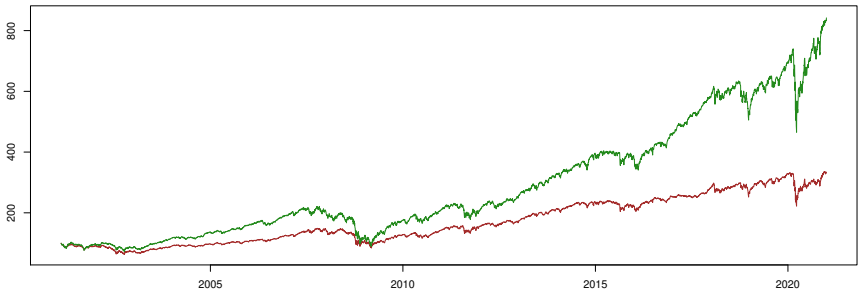

(a) *Portfolio Tracks*

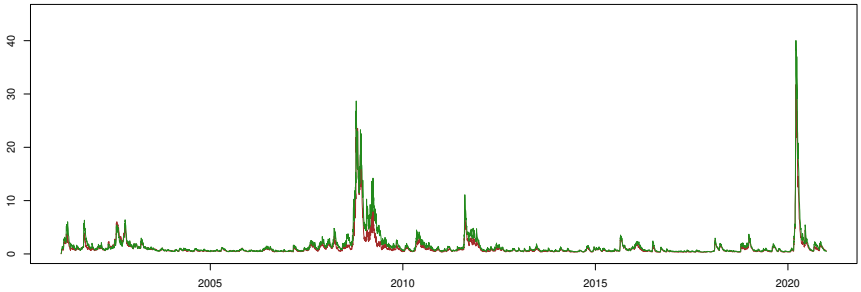

(b) *Conditional volatilities*

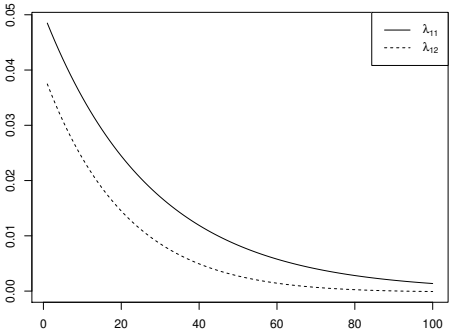

(c) *Response function of* $g_{B,t}$

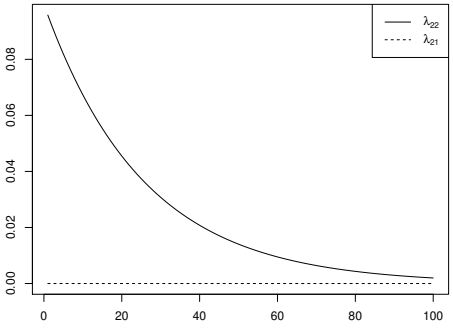

(d) *Response function of* $g_{G,t}$

Figure 14: *Performance, Conditional volatilities, and Response functions of Brown and Green portfolios formed on GMB4 criterion.*

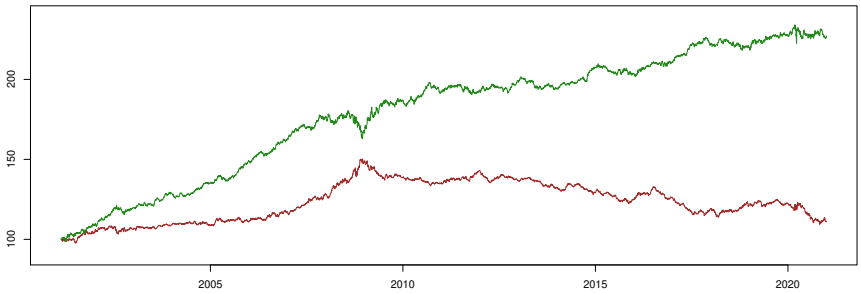

(a) *Portfolio Tracks*

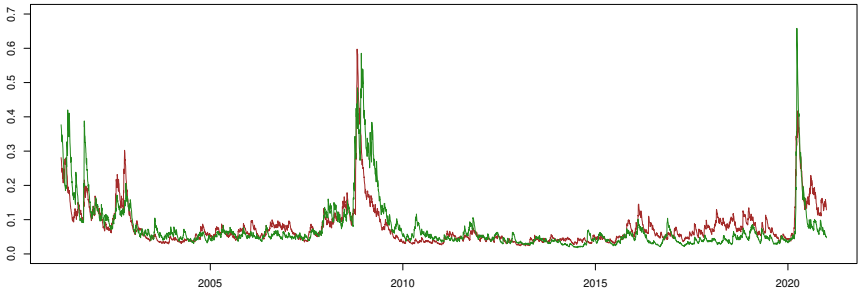

(b) *Conditional volatilities*

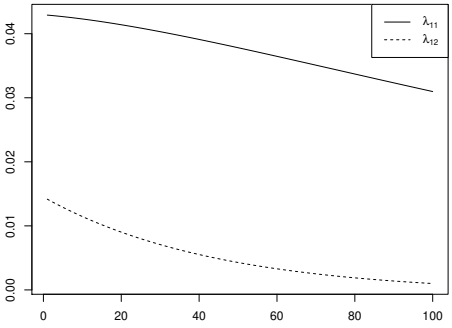

(c) *Response function of* $g_{B,t}$

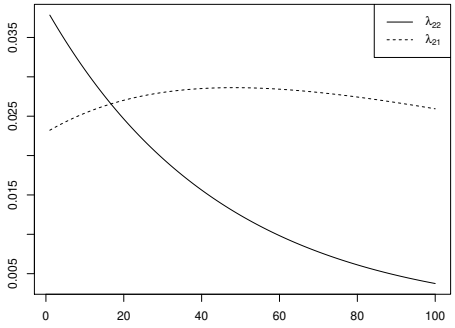

(d) *Response function of* $g_{G,t}$

Figure 15: *Performance, Conditional volatilities, and Response functions of Brown and Green portfolios formed on GMB4 criterion hedged of Fama French factors.*